INVESTIGATION OF THE X - RAY SHIELDING PROPERTIES OF CONCRETE CONTAINING LIME KILN DUST

THIS THESIS IS SUBMITTED TO UNIVERSITY OF GHANA, LEGON

BY

EMMANUEL KWAME AMPADU (10362490)

BSc PHYSICS (KNUST), 2010.

IN PARTIAL FULFILLMENT OF THE REQUIREMENT FOR THE AWARD

OF MPHIL APPLIED NUCLEAR PHYSICS DEGREE

JUNE, 2013.

DECLARATION

This is to certify that this thesis is the result of research undertaken by Emmanuel Kwame Ampadu towards the award of the Master of Philosophy degree in the Department of Nuclear Science and Application, School of Nuclear and Allied Sciences, University of Ghana.

…….. ……..

Emmanuel Kwame Ampadu Date

(Candidate)

…… ……

Prof. J.J. Fletcher Date

(Supervisor)

…….. ……..

Dr. K. A. Danso Date

(Co-supervisor)

DEDICATION

This work is dedicated to the Almighty God.

And to my family; Edward Ampadu Kumah, my dad, Regina Boah and Gertrude Mensah my mothers, Edward Adofo Kumah and Deborah Ampadu Kumah, my siblings.

And to all who find this work and its contents important and useful in one way or the other

ACKNOWLEDGEMENTS

I am eternally grateful to my supervisors, Prof J.J. Fletcher and Dr. K.A. Danso all of the Graduate School of Nuclear and Allied Sciences (SNAS), University of Ghana. This thesis would not have been possible without their help, patience and advice.

I also want to thank Rev. Dr. S. Akoto Bamful and Prof. S.B. Dampare all of SNAS for their useful suggestions and encouragement during this work.

Sincere thanks and gratitude goes to Dr. J.K Amoako, Head of the Health Physics and Instrumentation department of the Radiation Protection Institute at GAEC. I am also grateful to Mr. Collins Kafui Azah and Miss Veronica Afriyie Boahene all of the SSDL of the RPI at GAEC.

To Mawuli and Kwame of the Civil Engineering Laboratory of the GSB, many thanks to you for your immense help during the preparation of the samples as well as during the engineering tests. A big thank you to the workers at Carmeuse Lime (GH) Products.

To Mr. Daniel Nii Adjei and Miss Serwaa Yeboah, technologists at GAEC, thanks so much for your immense contribution and support during this work. I am very grateful.

To all my colleagues and friends especially Justice Darko, Nana Abena Kwansa, Rhoda Agyei Boateng, Phylicia Asibu, Jonathan Adu Adjei and my roommate, Robert Nunoo. Thank you for all the support and help.

To you all I offer my heartfelt sincere gratitude and thanks. May the Almighty God replenish all that you lost and continue to shower his blessings on you all.

TABLE OF CONTENTS

LIST OF FIGURES

LIST OF TABLES

ABSTRACT

An x-ray dose above the maximum permissible limit is harmful to human beings. A study of x-ray attenuation by materials is an important subject in protecting humans from harmful effects of radiation. Thus it is desirable to have knowledge about materials for effective x-ray shielding. Concrete is the most widely used construction material for this purpose and its composition plays an essential role in modifying the mechanical properties which affects significantly the shielding properties. This study summarizes the results of investigation carried out on concrete containing lime kiln dust, LKD in varying proportions. The objective of this research was to investigate the effects LKD has on the mechanical and shielding properties of concrete using it as part replacement material for cement. Compressive strength, flexural tensile strength, modulus of elasticity, unit mass and density were the mechanical properties investigated whilst linear and mass attenuation coefficients, half and tenth value layers and mean free path investigated for the shielding properties. The ability of concrete to attenuate x-ray intensity is assessed using its mass attenuation coefficient. The average mass attenuation coefficient for 100% concrete at 80 kVp was (0.1529 ± 0.0226) cm^2g^{-1}. At the same energy, 90% cement, 10% LKD concrete which had the highest density of (2.4622 ± 0.0218E-3) gcm^{-3} recorded an average mass attenuation coefficient of (0.1454 ± 0.2157) cm^2g^{-1}. The average density for all the concrete types was (2.4093 ± 0.4089E-3) gcm^{-3}. It was observed that increasing LKD ratio affected mechanical and shielding properties of concrete hence for x-ray facilities such as in hospitals and laboratories, LKD can be included in the cement mix used for plastering to form a multilayer aiding in attenuation.

CHAPTER ONE

1.0 INTRODUCTION

1.1 Background

When photons are directed unto an object, some are absorbed and scattered. Others completely penetrate the object unaffected. This is known as transmission. The penetrating ability of photons (x-rays and gamma rays) and other forms of radiation is one of the characteristic features that make them useful for medical imaging and other purposes. The penetration can be expressed as the fraction of radiation passing through the object.

Attenuation is the gradual loss in intensity of any kind of flux as it traverses a medium. The quantity of photons attenuated depends on the energy of the individual photons, density, elemental composition and thickness of the attenuator [1,2]. Attenuation is as a result of absorption and scattering. X-ray shielding is primarily based on the principle of attenuation.

Scientist observed that soon after the discovery of x-rays and other photons, exposure to large quantities of these ionizing radiations can produce lethal effects on the human body exposed as well as the environment as a whole [3].

Various materials when placed between a source and a detector, can affect the amount of radiation transmitted from the source to the detector. These effects are due to absorption of the emitted radiation in the source itself and attenuation in the material used for encapsulation of the source, or in a shielding barrier. Shielding is an important aspect of

radiation protection because it serves as a form of radiation control. The features of shields, their design, use and effectiveness warrant specific consideration [4].

Different forms of radiation require different shielding materials. Studies show that shielding design and shielding analysis are complementary activities. Shielding design seeks to determine the nature of the shield required to achieve a goal by identifying a source and specifying the target dose. In shielding analysis, the source and shielding are identified and the task is to determine the consequent dose [5].

Radiation shielding is based on two general classifications: thermal shielding and biological shielding. These consideration are for nuclear reactors and associated facilities, medical and industrial x-ray and radioisotope facilities and charged-particle accelerators where shielding is an important parameter. Thermal Shielding is used to dissipate excessive heat from high absorption of radiation energy, and Biological Shielding is needed to attenuate radiations to safe levels for humans, animals and the environment as a whole [6].

Work with any source of ionizing radiation (radioactive preparations, X-ray apparatus, accelerators, atomic and thermonuclear weapons) essentially presumes the safeguard of personnel and the immediate population from that radiation; this is often described as biological shielding [7].

For x-ray facilities, biological shielding is mostly considered since only a small fraction of the electronic energy is converted to x-rays and this can be ignored in heat calculation resulting in a less amount of heat being produced thus thermal shielding is not an option [8].

In most cases, high-density materials are more effective than low-density alternatives for blocking or reducing the intensity of radiation. However, a low density material can be used for effective shielding of x-rays once the material is made very thick [9].

Various materials can be used for photon shielding specifically x-rays. Notable among these materials are lead, tungsten and concrete. Lead and concrete are commonly used. Lead is often the material of choice used for x-ray shielding in medical and industrial x-ray facilities because of its high density of $11.35 gcm^{-3}$,high atomic number of 82, high level of stability, ease of fabrication, high degree of flexibility in application. Principally, it is effective at stopping x-rays.

Ordinary Portland Cement (OPC) concrete has been known for decades as a polyphase composite material for the purpose of radiation shielding [10]. The composite materials are made from chemically different and insoluble constituents. Concrete is a very good shielding material because it contains both the element hydrogen and heavy elements. The fact that its composition can vary makes it a versatile shielding material, in that, it can be changed to meet different situations. It has good mechanical strength and needs little maintenance [11]. The independent constituents retain most of their properties and therefore the composite material has better shielding qualities as it inculcates the individual properties into one.

Generally speaking, the denser the material, the thicker the material and the lower the x-ray energy, the greater the attenuation is [12]. To produce materials of very good qualities, it is useful to investigate how best a combination of materials into a single composite material can possess good structural and shielding properties.

Depending on the desired effects, a specified material can be made a part of a composite material to produce a new material of superior quality.

1.2 Problem Statement

Studies have shown that a dense shield material with a higher atomic number is a better attenuator of x-rays. Currently, the most widely used materials for photon (gamma and x-ray) shielding are lead, (Pb) and concrete.

Lead is the densest of the commonly available materials used for shielding with a density of 11350 kgm^{-3} whilst the density of OPC concrete is known to be in the range of (2240 – 2400) kgm^{-3} [13]. The compressive strength, flexural tensile strength and modulus of elasticity of ordinary concrete are also quoted to be in the range of (20 – 40) MPa, (3 – 5) MPa, and (14000 – 41000) MPa respectively [13].

The problem is to find a material which when added to concrete can relatively increase the density and appreciably improve the mechanical properties which can be used to replace lead and ordinary concrete in shielding photons specifically x-rays

1.3 Objectives

The main objective of this work is to investigate the best mix composition of lime kiln dust (LKD) ranging from 10% to 50% of the cement proportion as a component of concrete to determine their suitability and effectiveness for x-ray shielding.

Specifically, the following will be done:

- Determine the physical and mechanical properties such as mass, density, compressive strength, flexural tensile strength and modulus of elasticity of the

concrete containing Lime Kiln Dust (LKD) to know their suitability as structural material in building construction.

- Determine the radiation shielding properties: linear attenuation coefficient, mean free path, mass attenuation coefficient, half value layer and tenth value layer of the concrete containing LKD.

1.4 Relevance and Justification

There are several positive reports on radiation shielding properties of Lead and Ordinary Portland Cement (OPC) concrete containing other materials which have been used in concrete. Lead is readily available, and easily fabricated [6]. However, there are two major disadvantages of using lead for radiation shielding. First, it is its toxicity and its heavy mass. Secondly, it is also expensive, not mined, not milled or processed in Ghana.

Concrete is a composite construction material made primarily with aggregate (coarse and fine), cement, and water. The coarse aggregates are gravels whilst the fine aggregates are sand. Cement which is a primary component of concrete has seen remarkable increase in price on the Ghanaian market in recent times.

Due to the increase in price of cement and the fact that the composition of concrete can be varied, LKD has been added to the composition of concrete thereby reducing the percentage of cement in concrete.

It is therefore relevant and necessary to study LKD as an alternative material to be included in concrete composition for their suitability and efficiency as x-ray shielding materials with improved shielding properties to use at a lower health, environmental and

financial cost compared to lead and concrete. This is also in line with the fact that many radiological facilities will be built and shielding will play a very important role.

A successful research work shall produce a concrete based material that will be a solution to the challenges of radiation shielding at x-ray facilities. The outcome of this work will create beneficial use of the by-product from limestone production in Ghana thus contributing to national development.

1.5 Scope of work

During this research, lime kiln dust (LKD) has been included as a component of concrete to determine the appropriateness and efficiency as x-ray shielding material. This has been done by measuring properties such as linear attenuation coefficient, half value layer at different x-ray energies which include diagnostic x-ray energies, density, compressive strength and flexural tensile strength of the prepared shielding material. These properties have been chosen because they adequately describe a good shielding material. LKD has been selected because it is cheap, readily available and has an appreciable density.

The photons studied are x-rays with energies which encompasses typical x-rays for diagnostic purposes as this is in line with the fact that more medical facilities which include x-ray set-ups are being constructed as part of national development.

In this work, concrete made up of one part of cement, two parts of sand, four parts of gravels and water will be mixed. These ratios can either be by weight or by volume. For the purposes of this work, the ratio of the cement, LKD, sand and gravels are by weight whilst the ratio of the water is by volume.

The one part of cement in the mixture will be varied in different proportions ranging from 10% to 50% with LKD to determine their appropriateness and efficiency as radiation shielding material.

This has been done by measuring properties such as linear attenuation coefficient, mean free path, mass attenuation coefficient, half value layer and tenth value layer at different x-ray energies ranging from 80 kVp to 250 kVp.

The energy range selected is the range for industrial x-rays and they encompass the energy range for diagnostic x-rays. Mass measurement, compressive strength test, Density, flexural tensile strength and modulus of elasticity calculations will also be obtained.

These properties have been selected because they adequately describe a material good enough for x-ray shielding and for structural purposes.

1.6 Structure of thesis

This thesis is presented in five (5) chapters.

Chapter one (1) of this work gives the general introduction of this research work. It outlines the general background of the research, problem statement, objectives, relevance and justification and concludes with the scope of work.

Chapter two (2) reviews relevant and pertinent literature that aids a proper and good understanding of this research. It streamlines the context within which this work is carried out.

Chapter three (3) deals with the methodology employed in this research. This chapter describes and explains the various experimental procedures used in this thesis. Instrumentation and equipment used are also made mention of within this chapter.

In Chapter four (4), the results obtained are thoroughly discussed. This chapter is devoted to the discussion and comparison of the results obtained to similar works by other researchers.

Finally, Chapter five (5) of this thesis is the concluding chapter. It summarizes the work done and draws relevant conclusions and recommendations.

Following chapter 5 are references and appendices.

CHAPTER TWO

LITERATURE REVIEW

Sources of ionizing radiation have been in existence for technological ages. The natural and artificial sources are the major sources of radiation [14]. These ionizing radiations have found applications in different facets of human endeavour which include medicine, research, industry and agriculture [15].

In the design and construction of installation housing high intensity radiation sources and other generating equipments, a variety of shielding materials are used to minimise exposure to individuals and the environment as a whole [16].

The goal of radiation shielding is to limit radiation exposures to members of the public and employees to an acceptable level [17].

2.1 Radiation

Radiation is a general term applied to nuclear particles or electromagnetic waves, which are a direct or indirect result of radioactive decay and fission. Atoms with unstable nuclei are said to be radioactive. To attain stability, these atoms emit the excess energy or mass. These emissions are called radiations and can be electromagnetic like light or particulate, in which case mass is given off with the energy of motion. Gamma radiation and x - rays are examples of electromagnetic radiation. Gamma radiation originates from the nucleus while x - rays come from the electronic part of the atom. Beta and alpha radiation are examples of particulate radiation [18, 19].

2.2 Radiation shielding parameters

2.2.1 Attenuation coefficients

The understanding of interaction of photons with matter is an important parameter in various fields of radiation application and protection such as nuclear, medical and space physics. The principal modes by which photon interact with matter to be attenuated are by photoelectric effect, Compton Effect and pair production [20].

Radiation shielding is based on the principle of attenuation, which is the ability to reduce a wave's effect by blocking or bouncing particles through a barrier material. Charged particles may be attenuated by losing energy to reactions with electrons in the barrier. Neutrons can be made less harmful through a combination of elastic and inelastic scattering, and most neutron barriers are constructed with materials that encourage these processes [21].

If the interactions are of the "all-or nothing" type, then the attenuation of a beam of particles with identical energies all travelling in the same direction is described by an exponential law.

If at some distance into the material, N_0 particles are moving through a slab of material, then after penetrating an extra distance x it is found that the number of particles in the beam is reduced to:

$$N_{(x)} = N_o e^{-\mu x} \quad \ldots\ldots\ldots\ldots\ldots\ldots\ldots \quad (2.1)$$

This exponential attenuation law follows from the fact that, over any short distance, the probability of losing a particle from the beam is proportional to the number of particles

left. The quantity, μ, is known as the linear attenuation coefficient which is a measure of how rapidly the original photons are removed from the beam and also represent the combined photoelectric, Compton and pair production effects.

A large value of μ means that the original photons are removed after travelling only a small distance, *x*. The magnitude of μ depends on the incident photon energy, the chemical structure and bonding in the absorbing material and parameters such as thickness and density [22, 23].

Another attenuation parameter is the mass attenuation coefficient. The mass attenuation coefficient describes the total reduction in energy of x - ray and gamma radiation at a detector primarily due to both energy absorption and scattering.

Mass attenuation coefficient is defined as the measure of the average number of interactions between incident photons and matter that occurs in a given mass-per-unit-area thickness of material traversed [24].

The quantity of photons reaching a detector decreases as the mass attenuation coefficient increases for the same shield thickness and photon energy. Mass attenuation coefficient is likely to increase with increasing atomic number at the same photon energy, so materials with high atomic numbers and hence high mass attenuation coefficients are normally chosen to shield x – ray and gamma radiation [24, 25].

The relationship between the mass and linear attenuation coefficients is:

Mass Attenuation Coefficient (μ_m) = Linear Attenuation Coefficient (μ) / Density (ρ).

Mathematically,

$$\mu_m = \frac{\mu}{\rho} \quad \ldots\ldots\ldots\ldots\ldots\ldots\ldots\ldots\ldots (2.2)$$

Linear attenuation coefficient has units of per metre or per centimetre (m^{-1} or cm^{-1}) whereas mass attenuation coefficient has SI unit of metre squared per kilogram (m^2kg^{-1}) with centimetre squared per gram (cm^2g^{-1}) as one of its common units.

2.2.2 Mean Free Path (mfp)

Mean free path is the average distance a photon (x-ray) traverses between collisions. The range of a single photon in matter cannot be predicted, thus the average distance travelled before collision can be calculated from the linear attenuation coefficient [4, 5]. Mean free path is the inverse of attenuation.

Mathematically,

$$mfp = \frac{1}{\mu} \quad \ldots\ldots\ldots\ldots\ldots\ldots\ldots (2.3)$$

MFP is generally measured in units of distance. Either metres (m) or centimeters (cm)

2.2.3 Half Value Layer (HVL)

For a given material, the thickness of that material that attenuates 50% of the incident energy is known as the half-value layer (HVL). The concept of half-value layer **(**HVL) is used to quantify the ability of an x-ray beam to penetrate the material being examined.

The HVL of an x-ray beam is the thickness of any absorbing material that must be placed in the path of the beam to attenuate the transmission of the beam by one half.

The material primarily used to determine the HVL of diagnostic x-ray equipment is aluminum, thus HVL is sometimes expressed in terms of mm (millimeters) of aluminum.

Medical diagnostic x-ray machines typically have HVLs ranging from 2.3 to 5 mm Al.

HVL is given by

$$HVL = \frac{\ln 2}{\mu} \quad \ldots\ldots\ldots\ldots\ldots\ldots\ldots\ldots \quad (2.4)$$

Where μ is the attenuation coefficient

Approximate Half-Value Layer for Various Materials when radiation is from an x - ray Source are shown in table 2.1 [26, 27].

Table 2.1: A table comparing HVL values of ordinary concrete and Lead with increasing x-ray energy.

	Half Value Layer, mm	
Peak Voltage (kVp)	Lead ($\rho = 11.35 gcm^{-3}$)	Concrete ($\rho = 2.3\ gcm^{-3}$)
50	0.06	4.32
100	0.27	15.10
150	0.30	22.32
200	0.52	25.0
250	0.88	28.0
300	1.47	31.21

Materials of different compositions attenuate radiations to different degrees; therefore a convenient means of comparing the shielding performance of materials is needed.

The half-value layer (HVL) is usually used for this purpose and to evaluate what thickness of a given material is necessary to moderate the exposure rate from a source to some level.

Like linear attenuation coefficient, HVL is also photon energy dependent. Increasing the penetrating energy of the beam of photons results in an increase in the material's half value layer [18].

2.2.4 Tenth Value Layer (TVL)

The thickness of a specified substance which, when introduced into the path of a given beam of radiation, reduces the radiation field quantity to one-tenth of its original value. TVL is given by;

$$TVL = \frac{\ln 10}{\mu} \quad \text{..... (2.5)}$$

Where μ is the linear attenuation coefficient.

TVL is expressed in units of Metres (m) or Centimeters (cm). [4].

2.3 Radiation shielding

Radiation shielding technology evolved from the beginning of the 20th century when radium emanations and low energy x-rays were the only concerns and the design methods were primitive. In the 21st century, radiation shielding needs a very diverse and computational technology design methods [5]. This is due to the in-depth knowledge gathered in the field of radiation shielding as well as the diverse radiations now known.

Radiation shielding is the preferred method for safe working conditions in radiation environment. The amount of shielding required depends on the type of radiation being shielded, the radiation source and the dose rate that is acceptable outside the shielding barrier [28].

2.3.1 Types of radiations that can be shielded

Radiations of all types can be shielded. Gamma-rays and x-rays are attenuated by processes which are functions of atomic number and mass. Therefore, gamma radiation are best absorbed by atoms with heavy nuclei; the heavier the nucleus, the better the absorption [29].

2.3.2 Methods employed in shielding

The radiation protection principle that summarizes the safe use of radiation to derive a lot of benefits is known as low as reasonably achievable which states that radiation doses to persons involved in the use of ionizing radiation must be As Low As Reasonably Achievable (ALARA) [30, 31].

ALARA is ensured by three (3) principles;

- Time exposure which is the time an individual spends in the radiation environment must be minimized,
- Distance which obeys the inverse square law, $1/\ d^2$
- Shielding the sources of radiation from individuals.

A combination of any two or all three of these principles ensures an effective ALARA.The process of regulating the effects and degree of penetration of radioactive rays varies according to the type of radiation involved. Indirectly ionizing radiations, which include neutrons, gamma rays, and x-rays, are categorized separately from directly ionizing radiations, which involve charged particles. Different materials are better suited for certain types of radiation than others, as determined by the interaction between specific particles and the elemental properties of the shielding material.

2.3.3 Criteria for the selection of materials for shielding

An important aspect of the shield design process is to select the material or materials to be used. In making this selection, the physical processes of attenuation must be kept in mind, as well as the engineering problems associated. Some of the engineering problems include the compressive strength which gives the strength of the material and flexural tensile strength which is the ability of the material to resist deformation under load.

A variety of materials can be used for radiation shielding. To choose an appropriate type of shielding material; the type of radiation that is being shielded, the energy of the radiation, and the level of dose reduction need to be considered.

In choosing a shielding material, the first consideration must be effectiveness of the material to attenuate the incident radiations to its barest minimum. When dealing with external radiation protection, the most important consideration must be personnel protection. An effective shield will cause a large energy loss in a relatively small penetration distance without emission of more hazardous secondary radiations [32].

The thickness of a material to attenuate (shield) x-ray radiation is dependent upon the energy of the x-rays, the material's chemical composition and the material's density. The denser the material, the more radiation is attenuated.

The choice of the shield material is dependent upon many varied factors such as: ease of heat dissipation, resistance to radiation damage, multiple use considerations (e.g., shield and/or structural), uniformity of shielding capability, permanence of shielding and availability.

However, another factor which may also influence the choice of shielding materials is cost of the material. In shielding, cost is very important. Cost of materials must be balanced against the effect of shield size on other parts of the facility [21].

2.3.4 Materials for shielding

Interactions of various radiations with matter are unique as this determines their penetrability through matter and, accordingly, the type and amount of shielding needed for radiation protection.

Being electrically neutral, interactions of gamma rays with matter are statistical processes and depend on the nature of the absorber as well as the energy of the gamma rays. There is always a finite probability for gamma rays to penetrate a given thickness of absorbing material thus, unlike charged particulate radiations which have a maximum range in an absorber where all are stopped regardless of source strength, some gammas will always get through any thickness of absorber and, given a strong source, a lot more gammas may get through [4, 22]

The alpha particle is a positively charged helium nucleus which is completely stopped by 3 or 4 inches of air or a piece of paper. Beta particles are high speed electrons of varying energies. In general, they produce less ionization in matter than alpha particles but are more penetrating. Most common substances such as 1 inch of wood will completely absorb beta rays. Gamma radiation is emitted in all directions from its source as an expanding spherical front of energy, with great powers of penetration. High energy gamma radiation will not be wholly blocked by a foot of lead, while lower energy levels can be safely blocked by 3/16 inch or less of lead [21].

2.3.4.1 Lead

Lead is a chemical element in the carbon group with symbol Pb. Lead is a soft and malleable metal which is counted as one of the heavy metals.

The properties of lead which make it an excellent shielding material are its density, $\rho = 11{,}350\ kgm^{-3}$, high atomic number of 82, high level of stability, ease of fabrication, high degree of flexibility in application [33].

When applied as part of a neutron particle shielding system, lead has an extremely low level of neutron absorption and hence practically no secondary gamma radiation. If the shield material has a high rate of neutron capture, it will in time become radioactive, sharply reducing its effectiveness as a shield material. Being a metal, lead has an advantage over various aggregate materials such as concrete; being more uniform in density throughout. In addition, because commonly used forms of lead exhibit smooth surfaces, lead is less likely to become contaminated with dirt or other material which, in turn, may become radioactive [6].

2.3.4.2 Ordinary Portland Cement (OPC) Concrete

Concrete is a composite construction material composed primarily of coarse aggregates such as gravels, fine aggregates such as sand, cement, and water. The coarse and fine aggregates particles serve as a filler material to reduce the overall cost of concrete product as they are cheap, whereas cement is relatively costly. When these materials are thoroughly mixed and allowed to dry, it obtains a fixed shape of the container in which it was poured with a high strength. Concrete is a common large-particle composite in which both matrix and disperse phases are ceramic materials [34].

The average density of concrete falls in the range of 2.240 – 2.400 g/cm^3 with 2.3 g/cm^3 as its specific density. [13, 35, 36].

Concrete can be used for multiple purposes and it is commonly used as a radiation shielding material due to its cheap cost of production, availability of its material components, easier molded into complex shapes, good structural strength and suitability as photon shielding material compared to other shielding materials [37].

One component of concrete, Sand, has Silicon (Si) and Aluminum (Al) as its major elements with elements like Iron (Fe) and Magnesium (Mg) making up its minor elemental composition [34]. The sand fills the voids between the coarse particles.

Portland Cement is a hydraulic binder, that is, a finely ground inorganic material which when mixed with water, forms a paste which sets and hardens by means of hydration reactions and processes and after hardening, retains its strength and stability even under water [38].

In spite of this, the amount of cement-water paste should be enough to coat all the sand and gravel aggregates; otherwise the cementitious bonds will be incomplete.

Normally, ordinary Portland cement is rich in Calcium (Ca), Potassium (K), Silicon (Si), Aluminum (Al), Magnesium (Mg), Iron (Fe), Sulphur (S) and Manganese (Mn) [34].

High strength concrete mix is made up of one part of cement, two parts of sand, four parts of gravels and water. These ratios can either be by weight or by volume. For the purposes of this work, the ratio of the cement, Lime Kiln Dust (LKD), sand and gravels are by weight whilst the ratio of the water is by volume.

The above stated concrete mix ratio will give high strength concrete plus water tight properties making it great for ponds, and structural uses such as concrete panels and building slabs. [39, 40].

2.3.4.3 Concrete shield

For protection from x-rays occurring in nuclear reactors or high radioactive places a concrete with a unit density greater than 3200 kg/m^3 should be produced. A concrete with such properties can only be produced with the use of heavy aggregates or mixing cement with other materials [41].

Concrete is considered to be an excellent and versatile shielding material. It contains a mixture of various light and heavy elements and a capability for attenuation of photons and neutrons [42].

The ability of concrete to shield ionizing radiations is affected by its mass (or linear) attenuation coefficient. A higher mass attenuation coefficient implies a more efficient

concrete for shielding ionizing radiations. The attenuation coefficient of a material is dependent on the attenuation coefficients of its constituents [43].

Several studies conducted explain that major deterioration of concrete occurs after being exposed to high levels of radiation. It was concluded that fluxes ranging from (2×10^{19} to 2×10^{20}) neutrons/cm^2 damage concrete [44]. X-rays have a very low flux thus it has no long term effect on concrete.

2.3.4.4 Doped concrete shields

Various ways of reinforcing concrete are in use, thus various materials such as silica fume and fly ash as well as nano particles such as zinc and iron are added as a dispersed phase. Various studies have been conducted using different materials in concrete for radiation shielding. Some of these materials include Hematite, Barite, Colemanite and Boron – Carbide. The addition of these materials showed positive results for the attenuation of the radiations. Depleted uranium concrete (DUCRETE) has also been used for radiation shielding. Increasing the thickness of the material also reduces the intensity of the incident radiation [41, 45 – 47].

2.4 Lime

Lime is a general term for calcium-containing inorganic materials, in which carbonates, oxides and hydroxides predominate [48]. The word "lime" originates with its earliest use as building mortar and has the sense of "sticking or adhering". The rocks and minerals from which these materials are derived, typically limestone, are composed primarily of calcium carbonate. Limestone is a sedimentary rock composed largely of the minerals

calcite and aragonite, which are different crystal forms of calcium carbonate ($CaCO_3$). Limestone makes up about 10% of the total volume of all sedimentary rocks [41].

2.4.1 Limestone in Ghana

In Ghana, limestone production is done by Carmeuse Lime Products (GH) Limited. The very pure limestone that Carmeuse extracts to make lime is light to dark grey in colour with a $CaCO_3$ content of about 98% to produce calcium or dolomitic quicklime (CaO or CaO. MgO respectively).The pebble-lime thus produced is screened, crushed and finally stored. Two (2) products are mainly derived from limestone production; quick lime and hydrated lime with lime kiln dust (also known as enviro lime) as the by-product.

2.4.2 Descriptive analysis of each of the products of lime

2.4.2.1 Hydrated lime

Hydrated lime (Calcium hydroxide), traditionally called slaked lime, is an inorganic compound with the chemical formula $Ca(OH)_2$. It is a colourless crystal or white powder and is obtained when calcium oxide is slaked with water [49]. High calcium hydrated lime $Ca(OH)_2$ is a dry powder produced by reacting quicklime with a sufficient amount of water to satisfy the quicklime's natural affinity for moisture. The process converts CaO to $Ca(OH)_2$. The amount of water required depends on both the subtle characteristics of the quicklime and the type of hydrating equipment available. When heated to 512 °C, the partial pressure of water in equilibrium with calcium hydroxide reaches 101 kPa, which decomposes calcium hydroxide into calcium oxide and water [50, 51]

$$Ca(OH)_2 \rightarrow CaO + H_2O \quad \text{..... (2.6)}$$

Hydrated lime has a density of 2.211 g/cm^3 and a molar mass of 74.093 g/mol [52].

2.4.2.2 Quick lime

Calcium oxide (CaO), commonly known as quicklime or burnt lime is a widely used chemical compound. It is hard, white or grayish-white porous pebble or powder, odourless. It is soluble in water and glycerine but insoluble in alcohol [53].

Part of the extracted stone (limestone), selected according to its chemical composition and granulometry, is calcinated at about 1000°C in different types of kiln, fired by such fuels as natural gas, coal, fuel oil and lignite. The CO_2 of the stone is released to produce calcined dolomitic lime or quicklime (CaO. MgO or CaO respectively) [54].

According to the reaction:

$$CaCO_3 + heat \longrightarrow CaO + CO_2 \quad \text{..... (2.7)}$$

Quicklime is relatively inexpensive. It has a molar mass of 56.077 g/mol and a density of 3.35 g/cm^3 [53].

2.4.2.3 Lime kiln dust (Enviro lime)

Lime kiln dust (Enviro lime) is a by-product which is a mixture of quick lime, hydrated lime and other impurities. The chemical name is Calcium/Magnesium Carbonates and Oxides and belongs to the chemical family of Alkaline Earth Carbonates and Oxides. The chemical formula is

$$CaO + MgO + CaCO_3 \cdot MgCO_3$$ [55].

Lime kiln dust contains Calcium Oxide, CaO (Quicklime), Calcium Carbonate, $CaCO_3$ (Limestone), Magnesium Oxide, MgO (Periclase), Calcium Magnesium Carbonate, $CaCO_3 \cdot MgCO_3$ (Dolomite) and Crystalline Silica, SiO_2 (Quartz). All these elements are in variable concentrations with Quartz making up less than 5% of the total concentration.

Lime Kiln Dust, a product of the lime industry is the by-product of calcining limestone in rotary kilns. The gases and dust generated from this process are directed through a bag house where the dust is collected and the gases vented to the atmosphere. This dust material contains 15% to 18% Calcium Oxide, CaO, 70% to 75% Calcium Carbonate, $CaCO_3$, and the remaining portion is fly ash, which is high in silica and alumina [56]. Lime Kiln Dust (LKD) ranges from odourless to a slightly earthy odour, and is generally a white or grayish-white powder. In addition, lime kiln dust has the added benefit of stabilization. Lime kiln dust is alkaline, producing a PH of 12.4 in saturated solution. In addition to its obvious neutralizing potential, lime kiln dust also acts as a drying agent, forming calcium hydroxide when it comes in contact with water [56].

Preliminary measurements at the Chemistry laboratory of the Ghana Atomic Energy Commission showed that loose lime kiln dust has a density of 0.88 g/cm^3 and packed lime kiln dust has a density of 1.52 g/cm^3. Lime kiln dust is sold under the trade name of calciment.

2.4.3 Uses of the products from lime

Limestone has numerous uses: as a building material, as aggregate for the base of roads, as white pigment or filler in products such as toothpaste or paints and as a chemical feedstock.

2.4.4 Works with lime products and other materials

LKD is used for a variety of beneficial purposes, including soil conditioning and stabilization, industrial waste stabilization, Portland cement production, and agricultural uses. Unused LKD is usually stockpiled near the lime plant but can be disposed of in approved landfills. Hydrated lime is a very effective additive in bituminous asphalt. Lime substantially improves the cohesion of the components of asphalt, exhibiting excellent anti – strip characteristics and slows the aging process of the bitumen which results in less cracking. In masonry mortar, lime mortars harden more slowly than cement mortars but lime mortars have the advantage of greater plasticity making them easier to work with. They also have high flexural tensile strength while being more watertight, more elastic and less subject to cracking.

Products from lime effectively and quickly dry wet clays and silt soils and form a working table that provides a solid base for construction equipment traffic. They reduce the plasticity of clay soils, making it more crumble, improving its compaction characteristics and also added to react pozzolanically with soil to provide long term strength.

2.5 Effective Atomic Number, Z_{eff}

Effective atomic number signifies that at a given energy, photons would interact with a composite material in a similar way as a single element of atomic number equivalent to that composite material.

Z_{eff} represents radiation interaction with a matter and is a convenient parameter to consider in designing radiation shields, and computing absorbed dose, energy absorption

and build-up factor. Z_{eff} is not a constant for a given material but a parameter varying with photon energy which is dependent on the interaction processes involved [57,58].

A high-Z material effectively scatters protons and electrons. Each subsequent layer absorbs the X-ray fluorescence of the previous material, eventually reducing the energy to a suitable level. Each decrease in energy produces bremsstrahlung and Auger electrons, which are below the detector's energy threshold. Effective atomic number is an energy dependent parameter [59].

2.5.1 Computation of effective atomic numbers (Z_{eff})

Using the mass attenuation coefficient, μ_m of a material consisting of different elements, the effective atomic number Z_{eff} can be obtained by:

$$Z_{eff} = \frac{\sigma_a}{\sigma_e} \quad \text{..... (2.8)}$$

Where σ_a and σ_e are the effective cross-section per atom and the effective cross-section per electron, respectively and μ_m is the mass attenuation coefficient.

The total atomic cross-sections (σ_a) can be obtained using the relation

$$\sigma_a = \frac{1}{N_A} \frac{(\mu_m)_{concrete}}{\sum_i W_i/A_i} \quad \text{..... (2.9)}$$

Where N_A is the Avogadro's number and W_i is the fractional atomic mass of the elements.

For materials composed of multi-elements like concrete, the fraction by atomic mass is given by:

$$W_i = \frac{n_i A_i}{\sum_j n_j A_j} \text{ ……………………………….. (2.10)}$$

Where A_i is the atomic weight of the i^{th} element and n_i is the number of atoms present in a molecule.

The effective cross-section per electron (σ_e) is given by the formula

$$\sigma_e = \frac{1}{N_A} \sum_i \frac{f_i A_i}{Z_i} (\mu_m)_i \text{ ………………… (2.11)}$$

Where f_i is the number fraction of atoms of element i and Z_i is the atomic number of the i^{th} element in the mixture or compound, in this case concrete [58, 59].

2.6 Mathematical models for calculating shielding parameters

Monte Carlo simulation method is a numerical technique that, beside other applications, offers numerical solutions to radiation transport problems that are either too complex or impractical to be solved analytically. [45]

Monte Carlo N – Particles (MCNP) is an accepted code in handling radiation transport problem by the Monte Carlo technique. It is an industrial standard widely used by scientists and engineers. It tackles particulate interactions in a three (3) dimensional geometry [60, 61].

CHAPTER THREE

METHODOLOGY

This chapter gives an account of the scientific methods adopted as well as the equipment and instruments used to achieve the research objectives. It is divided into thematic areas, with each area addressing major aspects of the research.

3.1 Materials and Method

3.1.1 Sample Collection

The sand used for this work was collected from Amasaman, the capital of Ga West Municipal, a district in the Greater Accra Region of Ghana with geographical coordinates 5° 42' 0" North, 0° 18' 0" West. The area serves as one of the major sources of sand for construction in the Greater Accra region and beyond because of its large sand deposits.

Lime kiln dust came from Carmeuse Lime Products (GH) Limited in Takoradi. Carmeuse is located off the Takoradi – Accra road, close to Sekondi College. This is one of the major lime processing companies in the country.

Gravels were collected from kwabenya Aboum. Kwabenya is a village in the Ga East Municipal district, a district in the Greater Accra Region of Ghana with geographical coordinates 5°41′49″North, 0° 15′ 05″ West and serves as a very major source of gravels.

3.1.2 Sample excavation, collection and storage

A shovel was used to collect the LKD from the waste deposit site located on the premise of Carmeuse Lime Products (GH) Limited and placed in clean, dry, non-contaminated

and labeled plastic sacks. Sand from Amasaman was collected and stored in clean, dry, non-contaminated and labeled jute sacks. The gravels were also collected and stored in jute sacks. A bag of ordinary Portland cement (Ghacem) was purchased.

Upon collection of all of the materials, the samples were then transported to the Mechanical Engineering laboratory of the Ghana Standards Authority (GSA) where they were stored in a cool dry place under room temperature in readiness for preparation and studies.

3.1.3 Conditioning of samples

The sand was first washed with water to remove the dust after which it was allowed to dry in the sun. The dried sand was then weighed using an electronic balance. The other samples which include gravels, cement and Lime Kiln Dust (LKD) were also weighed with the electronic balance. The ratio for the mixing of the samples used was 1:2:4 for cement sand and gravels respectively.

These ratios were by weight where 1 part is equivalent to 4 kg. The proportion of water was measured using a measuring cylinder

One part of cement was varied in different proportions with LKD from 0% to 50 % in steps of 10%.

3.2 Fabrication of concrete into test pieces

For the engineering properties, such as density, compressive strength, flexural tensile strength and modulus of elasticity, cubes of dimensions $15\ cm * 15\ cm * 15\ cm$ were prepared. Slabs of dimensions $10\ cm * 10\ cm$ with varying thickness were also prepared

for radiation shielding tests. The field size of the x-ray source was taken into consideration in preparing the slabs for the shielding tests.

Out of each mixing ratio, 3 cubes for the engineering properties as well as two 1cm thick, one 3cm thick and one 5cm thick slabs were prepared.

The same procedure was followed for the other ratios but the material quantities were varied.

Table 3.1: Table showing the various quantities of materials used for each mixing ratio.

Concrete Type	Quantity of sand (kg)	Quantity of cement (kg)	Quantity of gravels (kg)	Quantity of LKD (kg)	Quantity of water (mL)
A	8.0	4.0	16.0	0.0	2000.0
B	8.0	3.6	16.0	0.4	2000.0
C	8.0	3.2	16.0	0.8	2500.0
D	8.0	2.8	16.0	1.2	2500.0
E	8.0	2.4	16.0	1.6	2500.0
F	8.0	2.0	16.0	2.0	2500.0

Where A is 100% cement, B is 90% cement, 10% LKD concrete, C is 80% cement, 20% LKD concrete, D is 70% cement, 30% LKD concrete, E is 60% cement, 40% LKD concrete and F is 50% cement, 50% LKD concrete.

Table 3.1 shows the exact quantity of materials used for each mixing ratio. The quantity of sand and gravels remained constant for all the ratios. The quantity of water was

increased from 2000 mL to 2500 mL in the 80% C, 20% L concrete ratio to 50% C, 50% L concrete ratio. This increase was to improve the workability of the concrete mix. This was due to the high affinity of the LKD for water in the mixture.

The materials were thoroughly mixed using a shovel. They were mixed on a wooden board to avoid losing some of the materials as they had been weighed. After the thorough mixing of the materials, some of the mixture was put in the metallic cube of dimensions $15\ cm * 15\ cm * 15\ cm$.

The metallic cubes and wooden slabs were oiled inside to prevent the mixture from sticking to the sides of the cube. The wooden $10cm * 10cm$ slabs of varying thickness were also filled with the mixture. They were then placed on a vibrator. It was vibrated to remove all the air bubbles trapped in the mixture and to properly compact the samples. The cubes and slabs were then allowed to stay in their containments for 24 hours. This was to allow for drying of the mixture as shown in Figure 3.1.

Figure 3.1: Concrete cubes and slabs after 24 hours

It was then removed from the containment, labeled and placed in a water bath filled with water to cure for 28 days as shown in figure 3.2. The labeling was to ensure easy identification. The samples were inspected on the 7^{th} and 14^{th} day.

Figure 3.2: Water bath containing labeled concrete cubes and slabs.

A veneer caliper was used to measure the thickness of the slabs to be used for radiation shielding tests after 28 days to get the true thicknesses of the slabs as concrete expands after curing.

3.3 Determination of the engineering properties

3.3.1 Density

After 28 days, the samples were taken out of the water. The densities were calculated based solely on the weight measurement of the cubes. The $15\,cm * 15\,cm * 15\,cm$ cubes were weighed on the electronic balance as shown in figure 3.3 and the average of the 3 cubes for each ratio calculated.

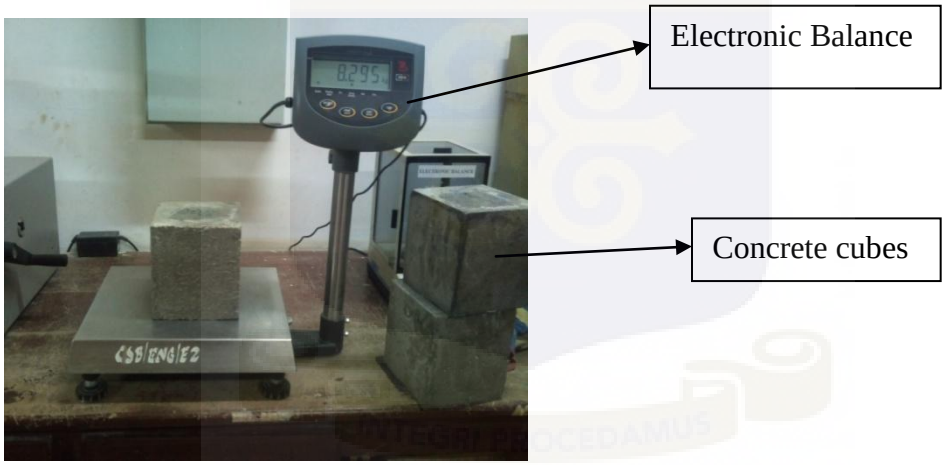

Figure 3.3 Electronic balance used to weigh concrete cubes.

The volume of each cube was calculated by using:

$$V = L^3 \quad \ldots\ldots\ldots\ldots\ldots\ldots [3.1]$$

Where

L is the length of one side of the cube.

The density in gcm^{-3} was calculated using as:

$$\rho = \frac{m}{V} \quad \ldots\ldots\ldots\ldots\ldots\ldots\ldots\ldots\ldots\ldots [3.2]$$

Where

ρ is the density in gcm^{-3}

m is mass of the test piece in g

V is the volume of the test piece in cm^3

3.3.2 Compressive Strength

Compressive strength is the capacity of a material to withstand uniformly directed pushing forces. In other words, compressive strength gives the actual strength of the concrete. Strength test results from cast cubes may be used for quality control, acceptance or rejection of concrete, or for estimating the concretes' strength in a structure.

For the purpose of this research, the cubes were subjected to compressive strength test. The average of 3 consecutive tests was performed for each mixing ratio. Figure 3.4 shows the compression testing machine.

A cube of each mixing ratio was placed in the compressor and a unilateral force applied. The force was increased steadily until a crack was seen in the cube as shown in figure 3.5. The value of force applied at which the crack was seen was recorded as the applied force.

Figure 3.4: Compression testing machine

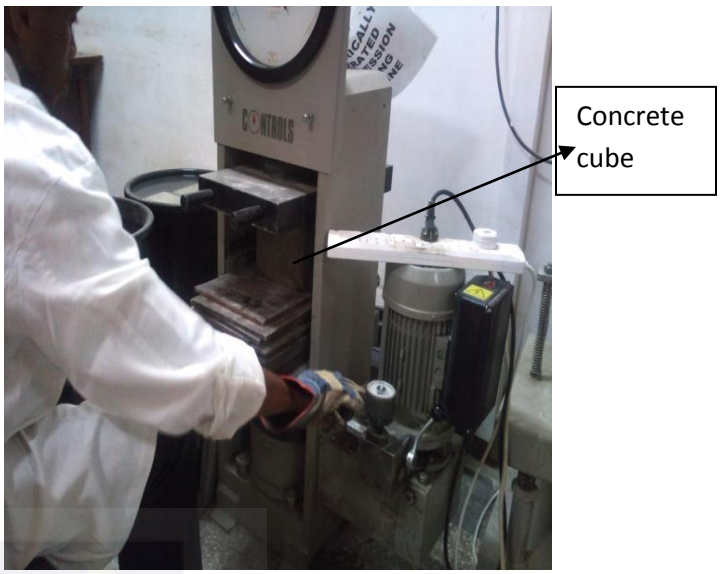

Figure 3.5: A concrete cube undergoing test

The procedure was repeated for the other two cubes for that mixing ratio. After the cracks increased in the cubes, the cubes crushed under increased force. Figure 3.6 shows the crushed cubes.

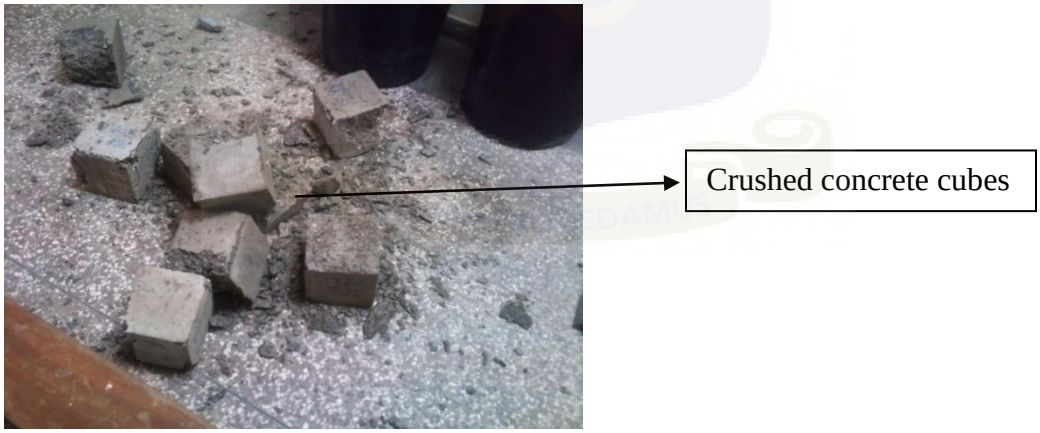

Figure 3.6 Crushed concrete cubes.

The recorded value on the scale of the compressor is then converted according to the equation

$$y = 0.7341x + 8.6877 \quad [3.3]$$

Where

y is the reference value in kN

x is the measured value in kN

This is the calibration equation for the compression testing machine captured in the calibration report of the Ghana Standards Authority, report number GSB/MET/114/IM/F015, with 12-06-2012 as the calibration date.

The compression testing machine used has a serial number of 03074239 with compression as its direction of force. It ranges from 0 – 2000 kN with 5 kN being its readability. The calibration of the compression testing machine was done at the civil engineering laboratory of the Ghana Standards Authority (GSA) in the following ambient conditions; temperature (27 ± 1) ^{o}C and relative humidity of 65 ± 5.

After conversion, the average force for each of the mixing ratio was calculated. The compressive strength was calculated as:

$$\sigma = \frac{F}{A} \quad [3.4]$$

Where

σ is the compressive strength in Nmm^{-2}

F is the force applied in N

A is the cross sectional area of the cube in mm^{2}

The cross sectional area of each cube was calculated as

$$A = L^2 \quad \ldots\ldots\ldots\ldots\ldots\ldots\ldots \quad [3.5]$$

Where

A is the cross sectional area of the cube in mm^2

L is the length of one side of the cube in mm.

Compressive strength can be measured in either Nmm^{-2} or MPa. In this work, the compressive strength was recorded in MPa. The conversion is 1 MPa = 1 Nmm^{-2}.

3.3.3 Flexural tensile strength

Flexural tensile strength is a material's ability to resist deformation under load. It is mathematically given by

$$Flexural\ tensile\ strength\ = 0.7(\sqrt{\sigma}) \quad \ldots\ldots\ldots\ldots\ldots\ldots\ldots\ldots\ldots\ldots\ldots\ldots \quad (3.6)$$

Where

σ is the compressive strength in MPa

3.3.4 Modulus of elasticity

This is the ratio of the applied stress to the change in shape of an elastic body. When a material is subjected to an external load it becomes distorted or strained. Within the limits of elasticity, the ratio of the linear stress to the linear strain is termed the modulus of elasticity or more commonly known as Young's Modulus. It is mathematically given by:

$$MOE = 4700(\sqrt{\sigma}) \quad \text{.....} \quad (3.7)$$

Where

MOE is the modulus of Elasticity

σ is the compressive strength in MPa

3.4 Determination of radiation shielding properties

3.4.1 Shielding set-up

The radiation source used is a PHILIPS MG324 constant potential x-ray machine used for calibration at the Secondary Standard Dosimetry Laboratory (SSDL) at Radiation Protection Institute (RPI) of the Ghana Atomic Energy Commission (GAEC). The PHILIPS MG324 was manufactured in Germany (Type 941 170 39522 and serial number 90 106 004).

In order to perform the shielding tests on the test pieces to determine their suitability for shielding x-rays, a survey meter, RADOS RDS – 120 Universal survey meter manufactured by RADOS TECHNOLOGY OY, FINLAND (serial number: 20563054) was placed at a fixed distance of 1m from the focus of the PHILIPS x-ray machine using a laser and a meter rule as shown in Figure 3.7. This is in accordance with the ISO 4037 recommendations.

A camera was placed on the screen of the survey metre.

From the console of the x-ray machine in the control room, exposure of x-rays was carried out in the SSDL at tube voltage of 80kV and tube current of 10mA without any concrete absorber between the source and detector. Fifteen readings were taken at 15 seconds interval from an LCD screen in the control room as shown in figure 3.8. The average of the 15 readings was then calculated to represent the dose reading for that kVp and current.

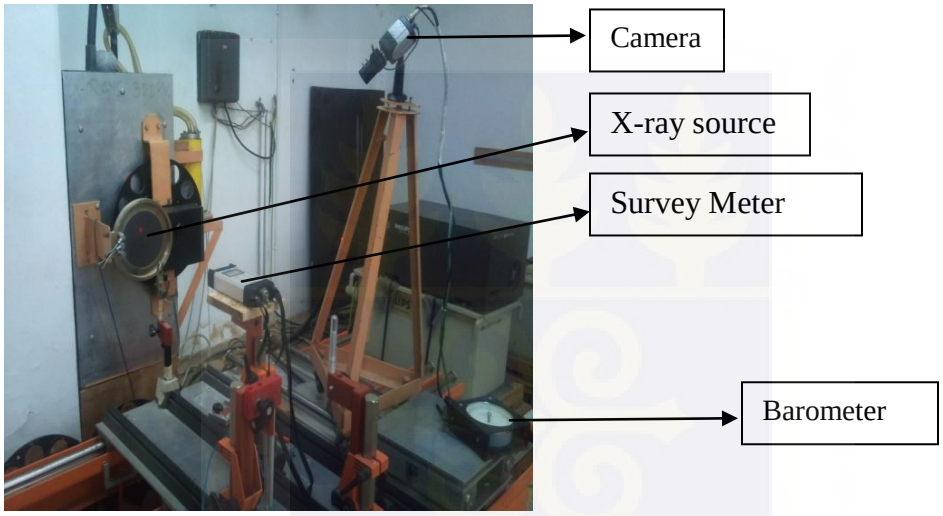

Figure 3.7: X-ray source and detector with no concrete slab

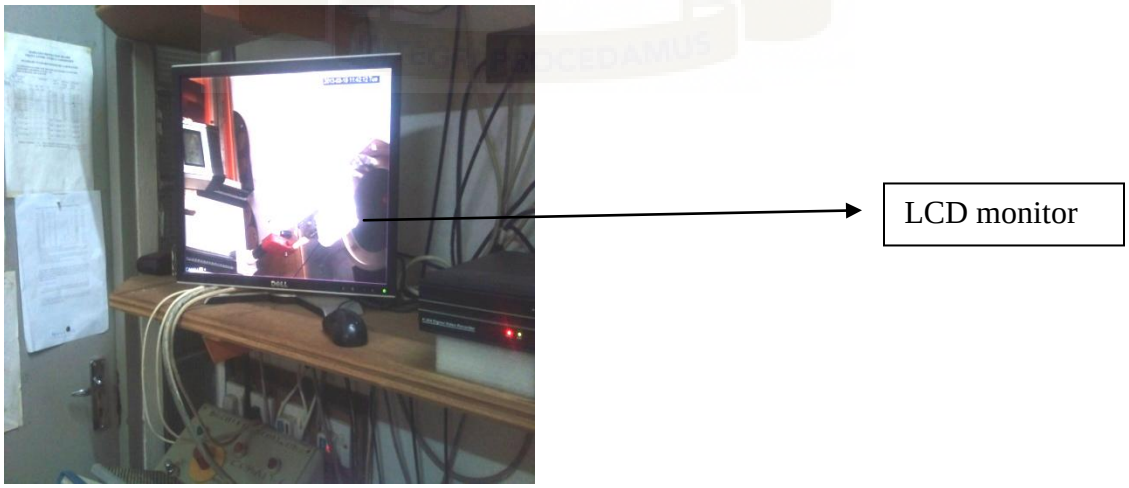

Figure 3.8: LCD monitor.

Concrete slabs of varying thicknesses were then placed between the x-ray source and the detector as shown in figure 3.9. Exposures were carried out and the doses registered by the survey meter recorded from the LCD screen at an interval of 15 seconds. Fifteen readings were taken and the average of the 15 readings was then calculated to represent the dose reading for that kVp, current and concrete thickness

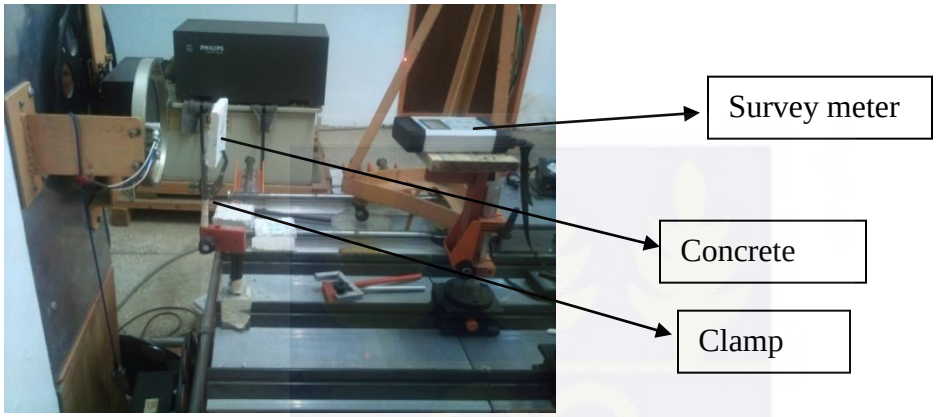

Figure 3.9: A concrete slab placed between the x-ray source and detector.

From the data obtained, a graph of dose rate, which was recorded by the survey meter in mSv/h, against thickness of concrete was plotted and from the plot the linear attenuation coefficient μ was calculated from which other important parameters such as Mean Free Path (mfp), mass attenuation coefficient (μ/ρ), Half Value Layer (HVL) and Tenth Value Layer (TVL) were calculated. The same procedure was followed to determine the linear attenuation coefficient at 100 kVp, 150 kVp, 200 kVp and 250 kVp all at a fixed tube current of 10 mA for all the concrete types.

For increasing thicknesses, individual thicknesses were clamped together to make up for the required thickness in the range. Leakage radiation was also measured and accounted for in the calculations.

An x-ray tube at a particular kVp generates a spectrum of energies thus additional filters were incorporated in the set up to ensure that the emitted x-rays from the tube at a particular kVp are approximately the exact energy.

Linear attenuation coefficient (μ) in cm^{-1}

The linear attenuation coefficient was calculated from the graphs plotted for each exposure and thickness of concrete slab. From the plot a curve of best fit was fitted from which an exponential function was arrived at. The exponential function is given by the equation (2.1)

$$N_{(x)} = N_o e^{-\mu x}$$

The constant, μ from the exponential function is the linear attenuation coefficient.

Mass attenuation coefficient in cm^2g^{-1}

From equation (2.2), mass attenuation coefficient is given by

$$\mu_m = \frac{\mu}{\rho}$$

μ = linear attenuation coefficient

ρ = Density

Calculation of the mass attenuation coefficient was done using the density of the various concrete ratios.

Mean Free Path (mfp) in cm

Mean free path is the average distance an x-ray photon traverses between collisions. Mean free path is the inverse of linear attenuation as shown in equation (2.3)

$$mfp = \frac{1}{\mu}$$

Where μ = linear attenuation coefficient

Half value layer (HVL) in cm

This is the thickness of concrete that will reduce the intensity of the incident radiation by one – half. HVL is a function of the linear attenuation coefficient. Recalling equation (2.4),

$$HVL = \frac{\ln 2}{\mu}$$

Where

μ = linear attenuation coefficient.

Tenth value layer (TVL) in cm

The thickness of concrete that will attenuate the incident radiation to one- tenth of the initial radiation is the tenth value layer.

Recalling equation (2.5), TVL is given by

$$TVL = \frac{\ln 10}{\mu}$$

Where

μ = linear attenuation coefficient.

3.5 Quality of result and statistics

3.5.1 Error estimation

For the sake of minimizing errors associated with the results, multiple readings were taken for each measurand under consideration. The arithmetic mean,$\bar{x}$ (average) of the readings was taken to represent the best value for the set of measurements. The standard deviation, σ, which specifies how the values deviate from each other, was also calculated. The following equations were used in calculating, $\bar{x}$ and σ:

$$\bar{x} = \sum_i^n \frac{X^n}{n} \quad \text{..... (3.3.1)}$$

Where

x = measured quantity

n = number of measurements

Standard deviation (σ) was used to find the error

$$\sigma = \sqrt{\frac{\sum(x-\bar{x})^2}{N}} \quad \text{..... (3.3.2)}$$

Where x = actual measured value

$\overline{x}$= mean of the measured values

N= number of measurements

3.5.2 Results validation and verification

The results obtained in this study were in all cases compared to those of standards and published results of similar works. These steps ensure the reliability of the experimental results.

CHAPTER FOUR

RESULTS AND DISCUSSION

The results of the various experimental works are presented and discussed within the framework of similar works in this chapter.

4.1 Engineering properties

4.1.1 Mass

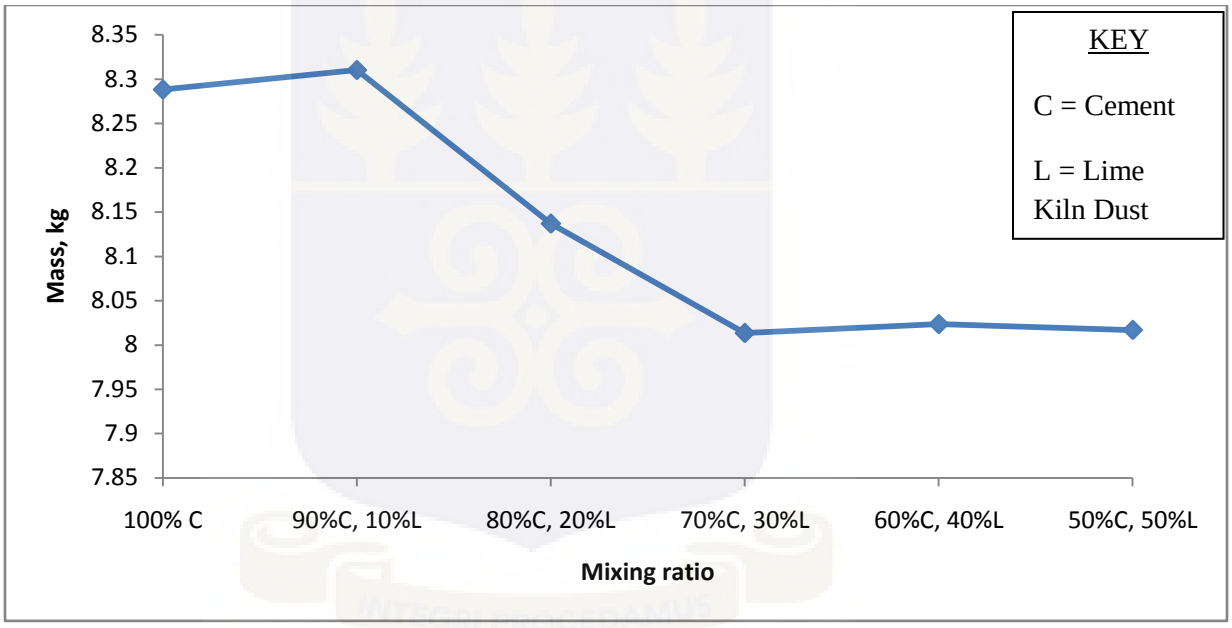

Figure 4.1: A comparison of mass of concrete cubes with different mixing ratios

In this study, the average mass together with the standard errors in kilogram (kg) of the cubes made of different percentages of cement and Lime Kiln Dust (LKD) were recorded as shown in Table 4.1.

Table 4.1: Table of average weight and calculated standard errors of the various concrete types

Concrete type	Mass (kg)	Standard Error (kg)
100% concrete	8.2880	0.0140
90% cement, 10% LKD	8.3100	0.0735
80% cement, 20% LKD	8.1367	0.0667
70% cement, 30% LKD	8.0133	0.0365
60% cement, 40% LKD	8.0233	0.0134
50% cement, 50% LKD	8.0167	0.0746

The recorded weight is the average weight of the 3 cubes.

From Figure 4.1, 90% cement, 10% LKD concrete cube has a slightly higher mass than 100% cement concrete. This implies that, as a small amount of LKD is added, approximately 10%, the mass slightly increases. This is evident in the fact that upon addition of more LKD and reduction of the cement content, the mass significantly decreases. This shows in the case of 90% cement, 10% LKD concrete to 70% cement, 30% LKD concrete. From 70% cement, 30% LKD concrete, the graph is a plateau where an increase in the LKD and decrease in the cement contents does not have any significant effects on the weight.

The loss in mass of the concrete cubes is attributed to the fact that there is excess lime, excess alkalis, excess Magnesium Oxide, MgO (Periclase) and excess Crystalline Silica, SiO_2 (Quartz) which are all part of the elemental composition of LKD [63].

Lime makes cement sound and strong, excess quantity makes the cement unsound, expands cement and breaks down the binding forces of the cement making the concrete mixture formed thereof weak resulting in loss of weight. Small quantity of Magnesium Oxide hardens concrete and gives cement its colour whilst excess Magnesium Oxide makes the cement unsound [63].

Unsound concrete is generally that concrete which emits a relatively hollow sound when a chain is dragged over its surface. They are generally loose, contaminated, weak, spalled and deteriorated.

For alkalis, small quantities are required as excess quantity results in efflorescence making the mixture weak and not compact enough, causing a loss in weight [63].

Any material containing Portland cement results in efflorescence, commonly known as salt bloom. The most common reaction occurs when calcium hydroxide (lime) formed in the hydration reaction of Portland cement is transported by water to the surface through capillaries in the concrete. There it combines with carbon dioxide from the air to produce calcium carbonate (an insoluble material) and water. Efflorescence can also be caused by hydroxides and sulfates of either sodium or potassium, which are much more soluble in water than calcium and they form efflorescence more rapidly than calcium hydroxide. These salts can come from cement, aggregates, water, or admixtures in this case LKD. While mostly cosmetic, in some cases it can lead to spalling and weakening of concrete or brick structures [64, 65].

4.1.2 Density

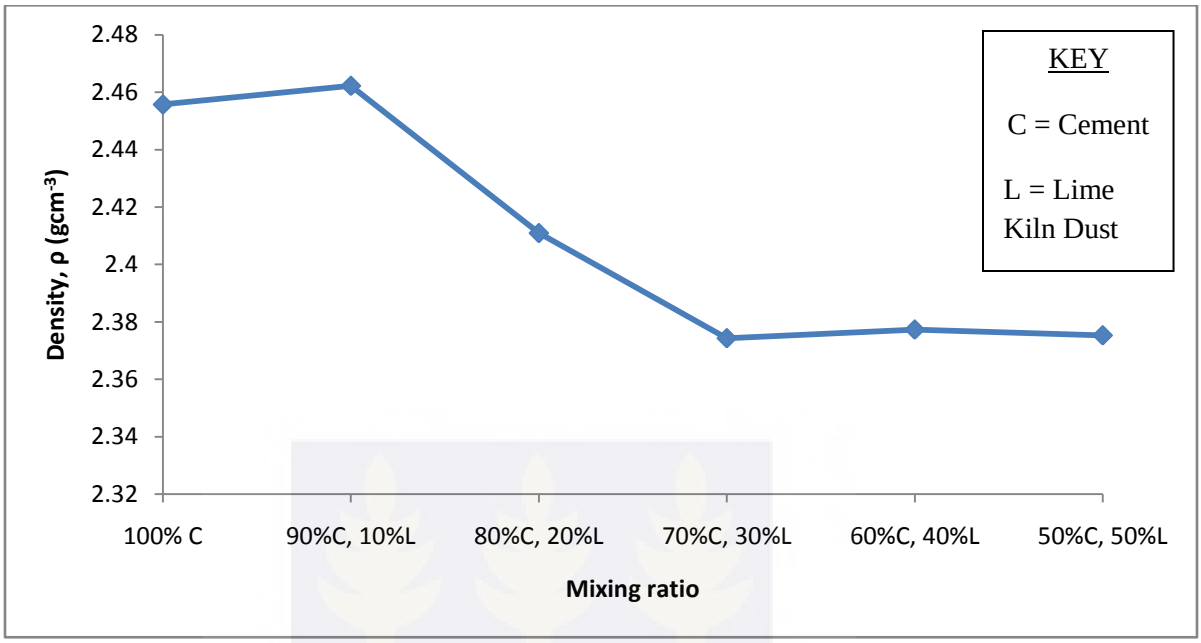

Figure 4.2: A graph comparing the density of concrete cubes with different mixing ratios

The average densities together with the standard errors of the cubes made of different proportions of cement and LKD in gcm^{-3} were recorded as tabulated in table 4.2

Table 4.2: Table of densities and calculated standard errors of the various concrete types

Concrete type	Density (gcm^{-3})	Standard Error (gcm^{-3})
100% concrete	2.4557	0.0041E-3
90% cement, 10% LKD	2.4622	0.0218E-3
80% cement, 20% LKD	2.4109	0.0198E-3
70% cement, 30% LKD	2.3743	0.0108E-3
60% cement, 40% LKD	2.3773	0.0040E-3
50% cement, 50% LKD	2.3753	0.0221E-3

These density values when multiplied by 1000, quotes the density values in kg/m^3. This yields figures that conform generally to the density range of 2240 - 2400 kg/m^3 [13]. 2300 kg/m^3 is the typical density of concrete [14]. The density of concrete is a measurement of concrete's solidity. The process of mixing concrete can be modified to form a higher or lower density of concrete end product.

From figure 4.2, 90% cement, 10% LKD concrete is seen to have a marginally higher density of 0.43% more than the 100% cement concrete. Generally, the results attained as shown in figure 4.2, indicates that the addition of LKD to concrete decreases the density. A slight LKD content of 10% in the mixture improves the density slightly. This is seen in the density value of 90% cement, 10% LKD concrete with its value quoted as 2462.2 kg/m^3 whereas 100% cement concrete has a density value of 2455.7 kg/m^3.

The density is seen to decrease from (2.4622 ± 0.0218E-3) gcm^{-3} for the 90% cement, 10% LKD to (2.3743 ± 0.0108E-3) gcm^{-3} for the 70% cement, 30% LKD concrete. As the LKD content in the concrete is increased, the binding properties are reduced making the concrete possess weaker bonds and subsequently reducing the weight of the concrete sample. Further addition of LKD to concrete does not greatly influence the density of the concrete as the graph takes a shape of a plateau. This trend is not surprising since density is calculated from the mass per unit volume and the masses for the test concrete cubes for the various mixing ratios followed the same trend.

4.1.3 Compressive strength

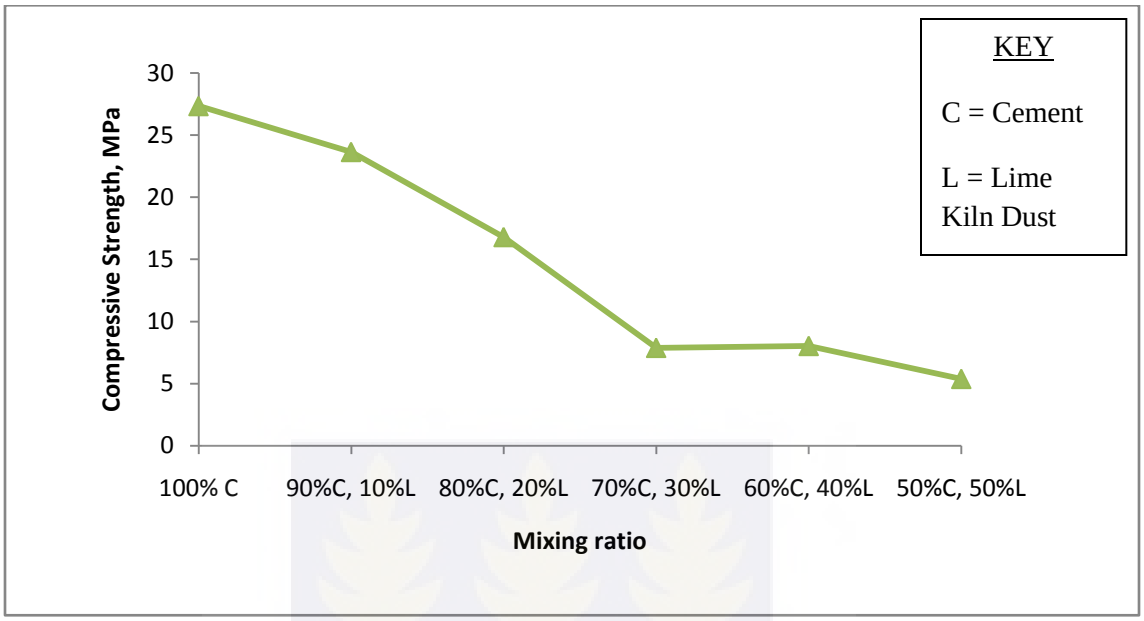

Figure 4.3: A graph comparing the compressive strengths of concrete cubes with different mixing ratios

Compressive strength is the capacity of a material or structure to withstand axially directed pushing forces. When the limit of compressive strength is reached, brittle materials are crushed. On an atomic level, the molecules or atoms are forced apart when in tension whereas in compression they are forced together [66].

In this study, the compressive strength together with the standard errors in MPa of the cubes made up of different proportions of cement and LKD were recorded and tabulated in table 4.3

Table 4.3: Table of Compressive strength and calculated standard errors of the various concrete types

Concrete type	Compressive strength (MPa)	Standard Error (MPa)
100% concrete	27.3575	0.0013
90% cement, 10% LKD	23.6598	0.0006
80% cement, 20% LKD	16.8082	0.0007
70% cement, 30% LKD	7.8903	0.0008
60% cement, 40% LKD	8.0425	0.0001
50% cement, 50% LKD	5.3889	0.0002

The compressive strength tests on the cubes were conducted after 28 days of curing.

Concrete compressive strength requirements can vary from 17 MPa for residential concrete to 28 MPa and higher in commercial structures [67]. Thus from table 4.3, the compressive strength for the 100% concrete and 90% cement, 10% LKD concretes fall within the range for commercial structures. An x-ray facility is a commercial structure.

From figure 4.3, there is a general decrease in the compressive strength of the concrete cubes from 100% concrete to 70% cement, 30% LKD concrete. There is a slight stability in the compressive strength of the concrete cube of 70% cement, 30% LKD and 60% cement, 40% LKD but then the strength massively decreases in the 50% cement, 50% LKD.

The strength of concrete is largely influenced by a lot of factors notable among them is the water – cement ratio and the quantity of cement in the mixture. The ratio of the water to cement is the chief factor for determining concrete strength. The lower the water-cement ratio, the higher is the compressive strength. A certain minimum amount of water is necessary for the proper chemical action in the hardening of concrete; extra water increases the workability but reduces strength [68].

This statement is validated in the sense that as the water content was increased with an increase in the LKD component, the strength of the concrete reduced.

The increase in water content enhanced the workability of the concrete but this also reduced the resultant compressive strength. The water content was increased in the 80% cement, 20% LKD concrete, 70% cement, 30% LKD concrete, 60% cement, 40% LKD concrete and 50% cement, 50% LKD concrete.

Concrete is mostly specified by strength. The strength is chiefly influenced by the amount of cement in the mix [69]. From figure 4.3, decreasing the cement content from 100% to 70% cement, caused the strength to decrease from 53.0568% to 13.5162% for 70% cement, 30% LKD concrete. There was a very slight increase of 1.9290% when the cement content decreased from 70% to 60% but this increase is insignificant due to the fact that the strength further decreases to 32.9947% of 60% cement, 40% LKD concrete when the amount of cement decreases from 60% to 50%.

Lime, (CaOH) is the main ingredient of cement, having about 60 % of the total ingredients. This percentage of lime imparts excellent cementing property, thus a

deficiency of lime causes a decrease in the strength of cement and a higher percentage of lime causes unnecessary expansion and disintegration of the cement and it cementing property. This explains why increasing the LKD proportions results in weak concrete.

4.1.4 Flexural tensile strength

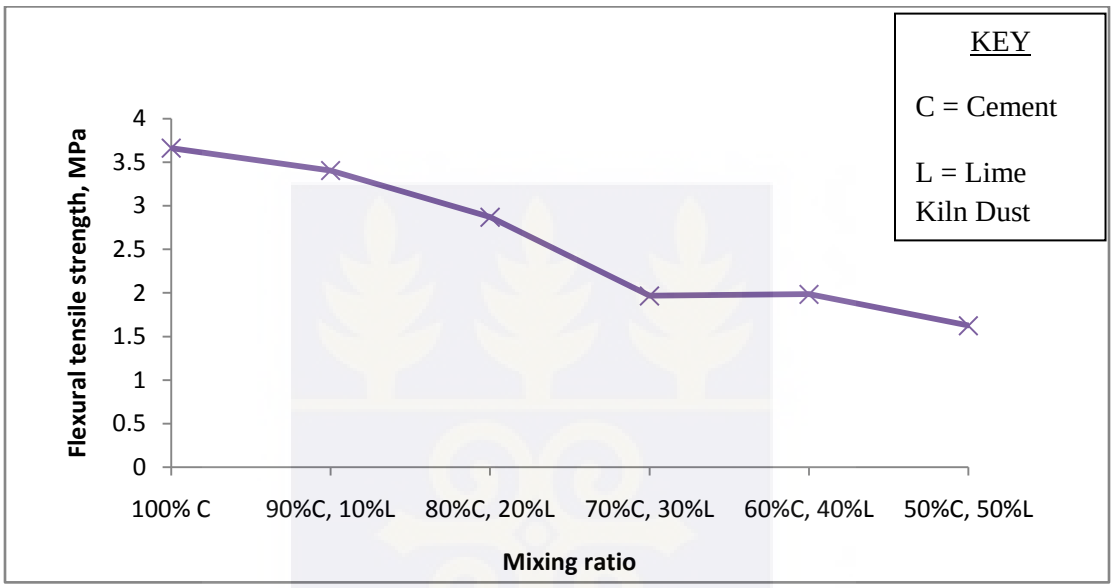

Figure 4.4: A graph comparing the flexural tensile strength of concrete cubes with different mixing ratios

Flexural strength, also known as modulus of rupture, bend strength, or fracture strength, is a mechanical parameter for brittle material, which is defined as a material's ability to resist deformation under load [70]. The flexural tensile strength enables the concrete material to resist the application of a tensile force. Withstanding the tensile force depends on the internal configuration of the material which provides the internal resistance to the applied force [34].

Flexural strength increases proportionally with compressive strength. Flexural strengths of interest fall in a range of 3.0 MPa to 5.0 MPa [13] for commercial and residential structures. Flexural tensile strength is about 10% to 20% of compressive strength depending on the type, size and volume of coarse aggregate used [71].

The flexural tensile strength together with the standard errors in MPa of the cubes made of different proportions of cement and LKD were recorded as shown in table 4.4

Table 4.4: Table of flexural tensile strength and calculated standard errors of the various concrete types

Concrete type	Flexural tensile strength (MPa)	Standard Error (MPa)
100% concrete	3.6613	0.0252
90% cement, 10% LKD	3.4050	0.0171
80% cement, 20% LKD	2.8698	0.0185
70% cement, 30% LKD	1.9663	0.0198
60% cement, 40% LKD	1.9852	0.0070
50% cement, 50% LKD	1.6250	0.0099

From the graph in figure 4.4, the flexural tensile strength decreases from the 100% concrete to 70% cement, 30% LKD, remains stable and further decreases to (1.6250 ± 0.0099) MPa representing the flexural tensile strength for 50% cement, 50% LKD.

Once the flexural tensile strength capacity of concrete has been exceeded, the concrete will crack [72].

4.1.5 Modulus of elasticity, MOE

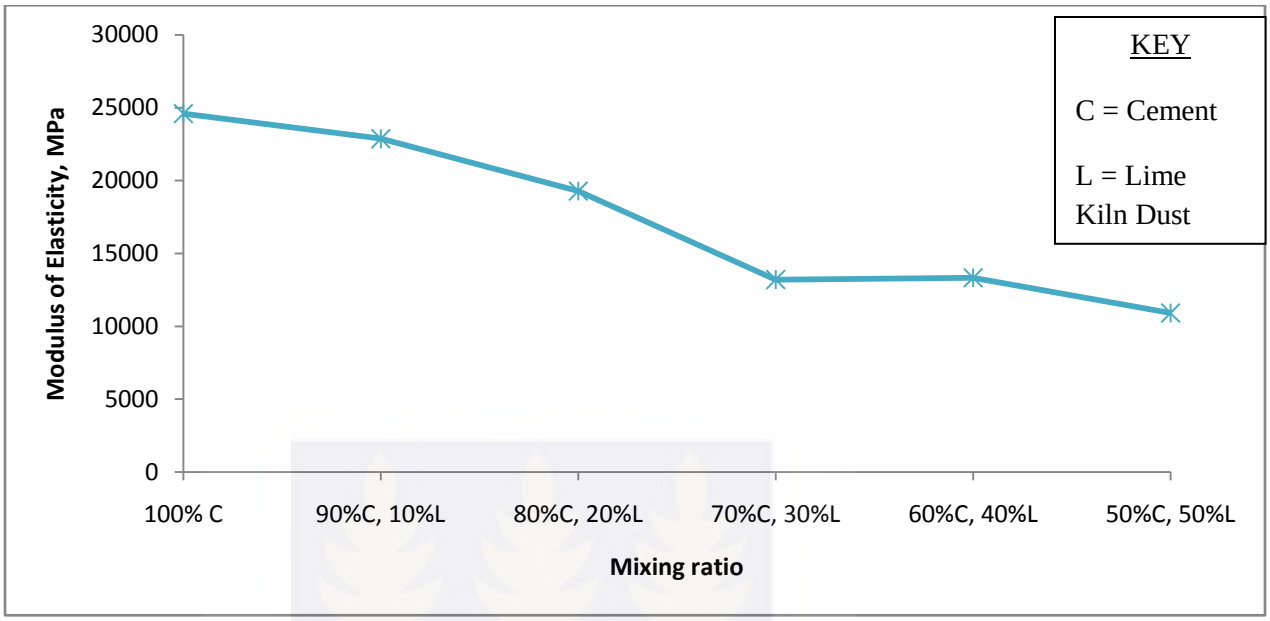

Figure 4.5: A graph comparing the modulus of elasticity of concrete cubes with different mixing ratios

Modulus of elasticity is the ratio of the applied stress to the change in shape of an elastic body. When a material is subjected to an external load it becomes distorted or strained. The modulus of elasticity, also called Young's modulus, E, is a material property, which describes its stiffness and is therefore one of the most important properties of solid materials. It is the tendency of a material to return to its original shape after deformation [73]

Mechanical deformation puts energy into a material. This energy is either stored elastically or dissipated plastically. A material's ability to store this energy is summarized in stress-strain curves. Stress is defined as force per unit area and strain as elongation or contraction per unit length. The higher the E-module, the higher peak stresses will

become. This means that the higher the E-module in concrete, the sooner cracks will appear [73].

The modulus of elasticity together with the standard errors in MPa of the cubes made of different proportions of cement and LKD were recorded

Table 4.5: Table of modulus of elasticity and calculated standard errors of the various concrete types

Concrete type	Modulus of Elasticity (GPa)	Standard Error (GPa)
A	24.5831	0.1695
B	22.8610	0.1151
C	19.2687	0.1244
D	13.2021	0.1329
E	13.3289	0.047
F	10.9106	0.0665

Where A is 100% concrete, B is 90% cement, 10% LKD concrete, C is 80% cement, 20% LKD concrete, D is 70% cement, 30% LKD concrete, E is 60% cement, 40% LKD concrete and F is 50% cement, 50% LKD concrete.

There is a general decrease in the plot as shown in figure 4.5 from 100% concrete to 70% cement, 30% LKD concrete, it then stabilizes and further decreases to (10910.5821 ±

66.4680) MPa equivalent to 50% cement, 50% LKD concrete. This decrease is as a result of the weak inter-atomic bonds that exist in the concrete as the LKD content is increased.

These modulus of elasticity values when multiplied by 0.001, quotes the values in GPa. Concrete commonly has a modulus of elasticity in the range of 17 - 30 GPa [74]. This puts the modulus of elasticity of 100% concrete, 90% cement, 10% LKD concrete and 80% cement, 20% LKD concrete within the range specified. The exact value of modulus of elasticity depends on the concrete's uniaxial compressive strength after 28 days of curing [74].

4.2 Shielding properties

4.2.1 Attenuation

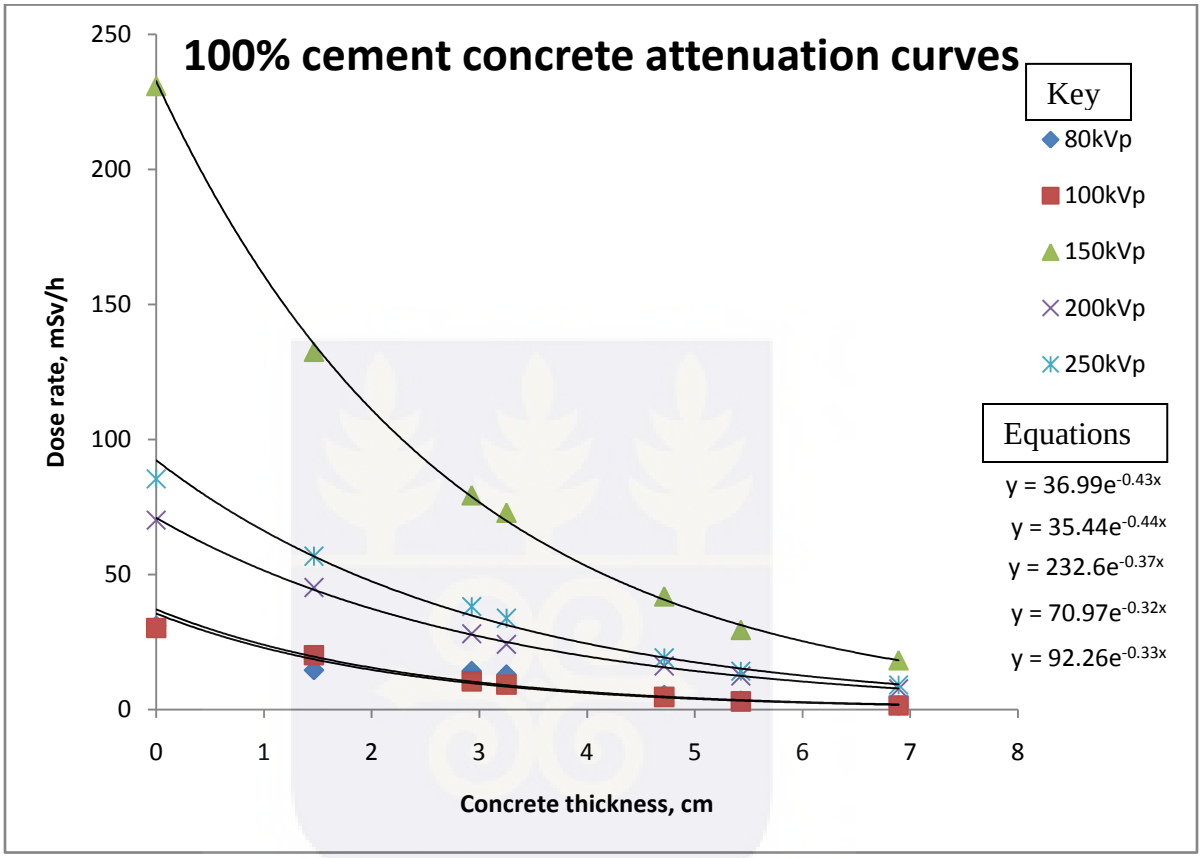

Figure 4.6: A graph of concrete thickness against dose rate for 100% concrete.

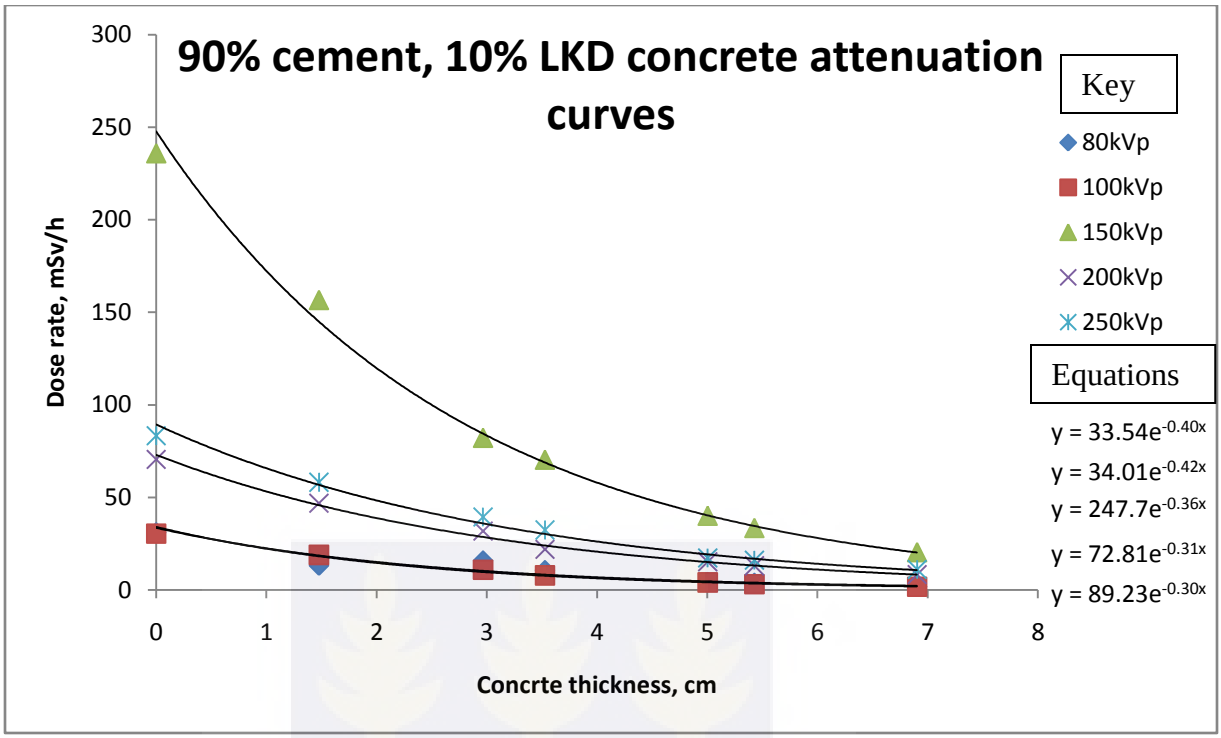

Figure 4.7: A graph of concrete thickness against dose rate for 90% cement, 10% LKD concrete.

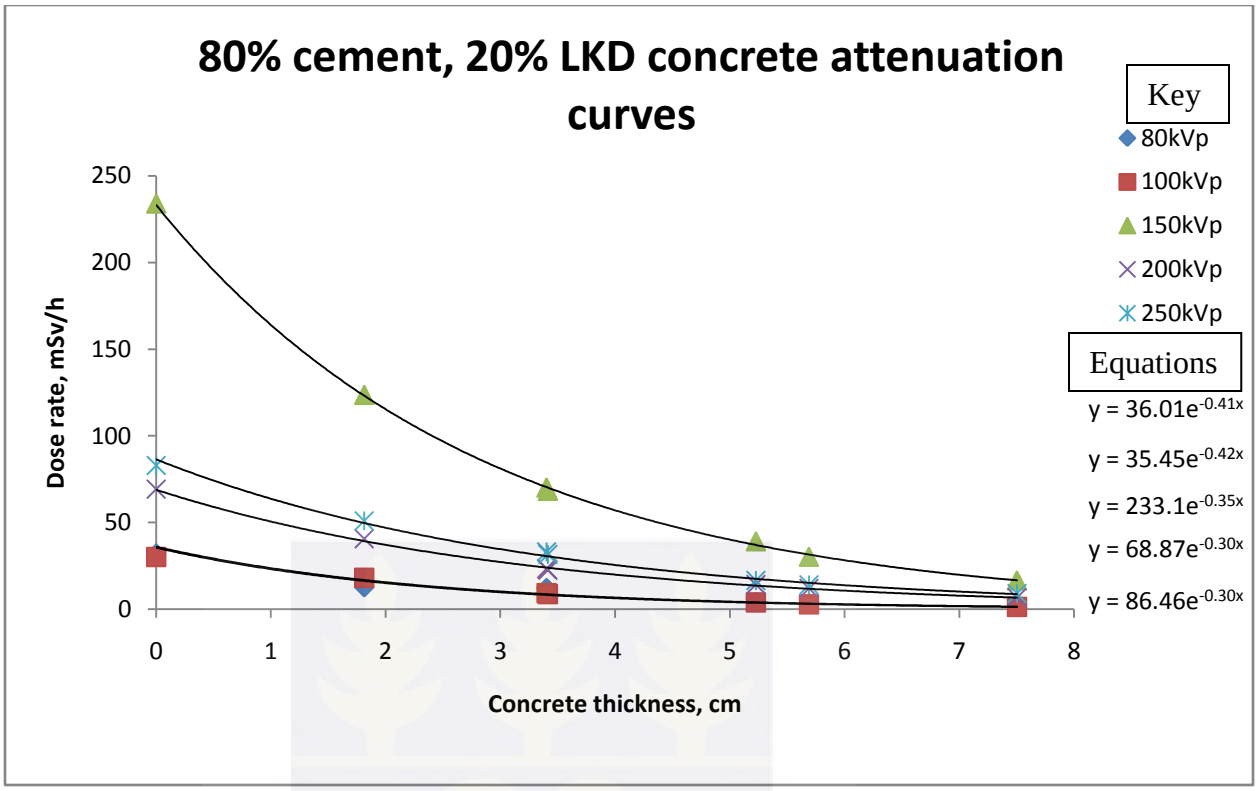

Figure 4.8: A graph of concrete thickness against dose rate for 80% cement, 20% LKD concrete.

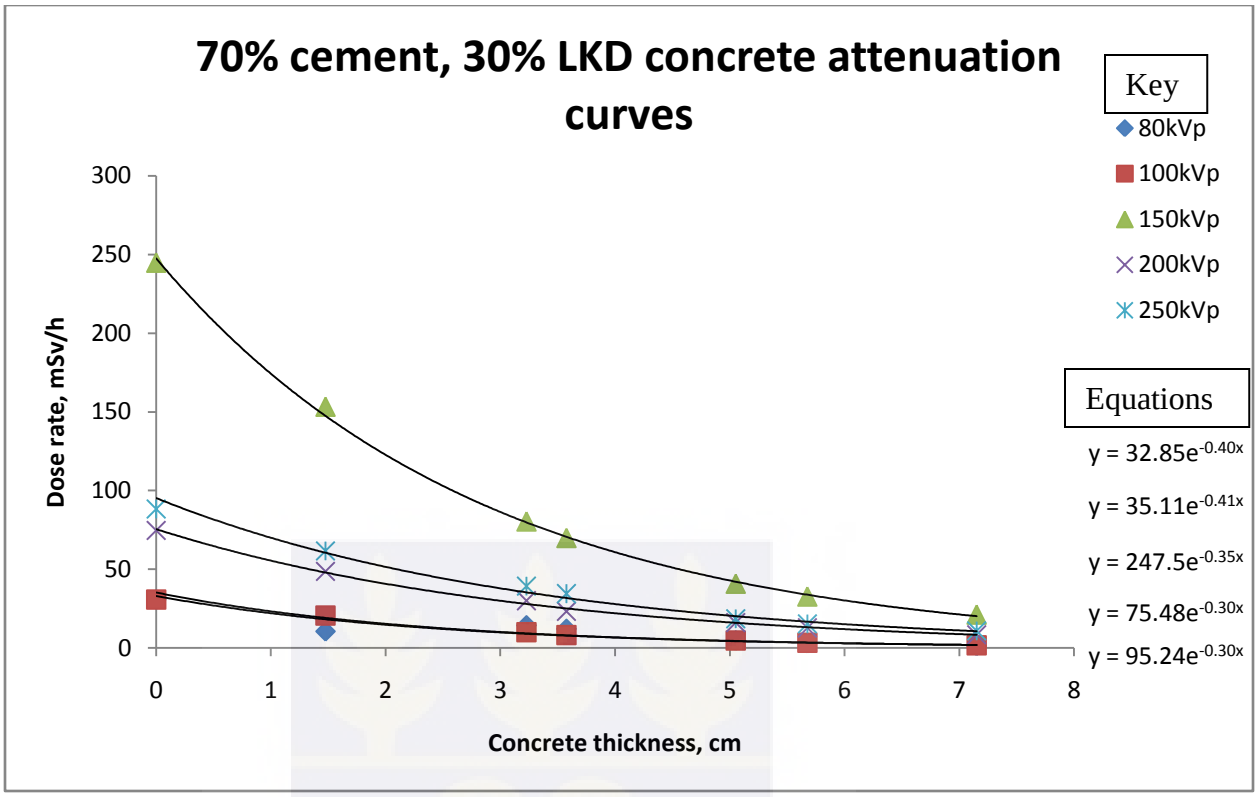

Figure 4.9: A graph of thickness against dose for 70% cement, 30% LKD concrete.

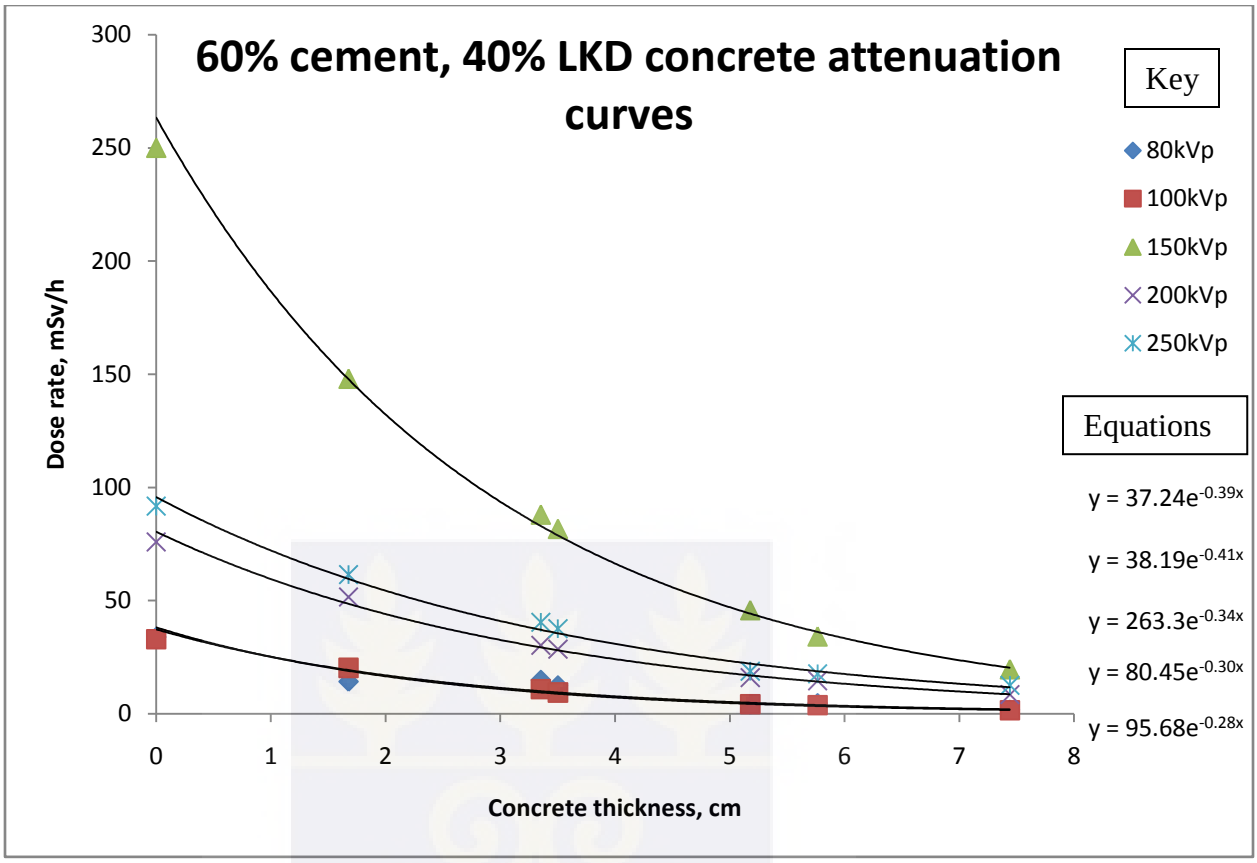

Figure 4.10: A graph of concrete thickness against dose for 60% cement, 40% LKD concrete.

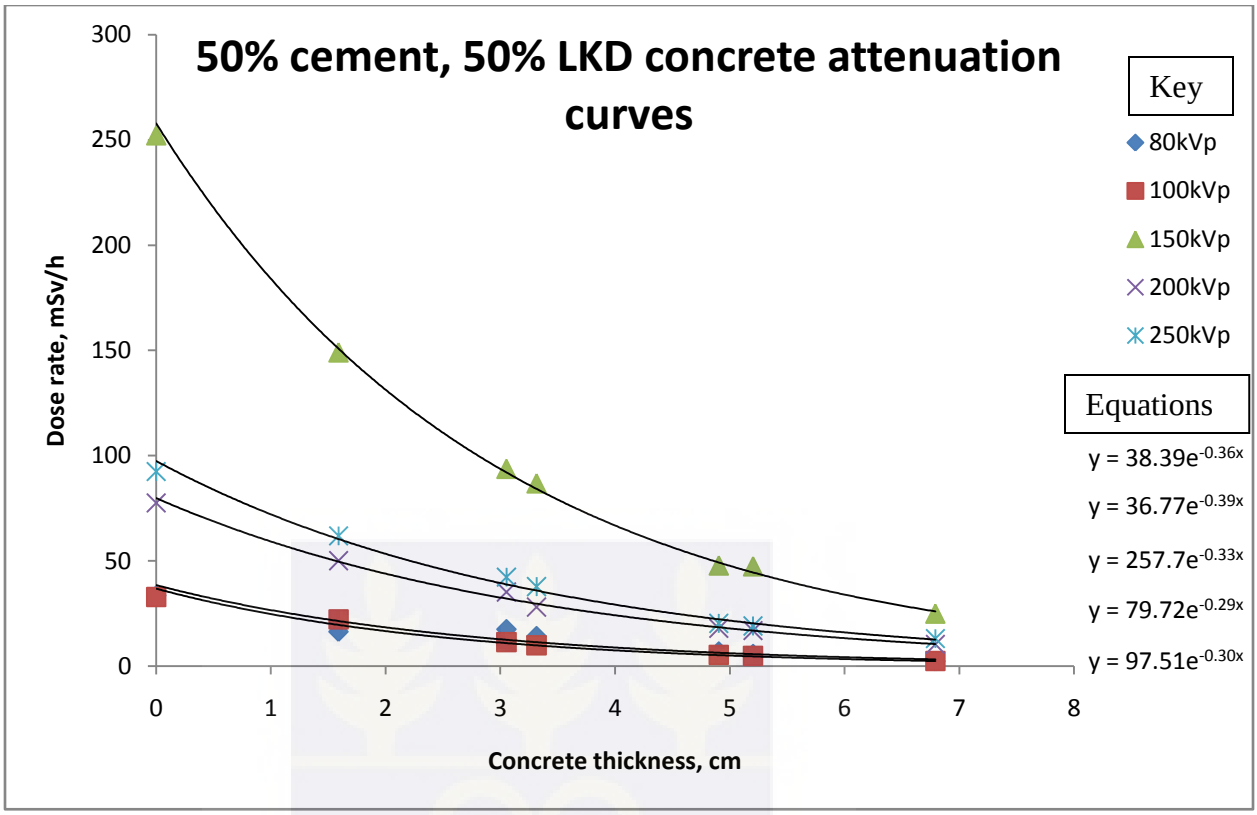

Figure 4.11: A graph of concrete thickness against dose for 50% cement, 50% LKD concrete.

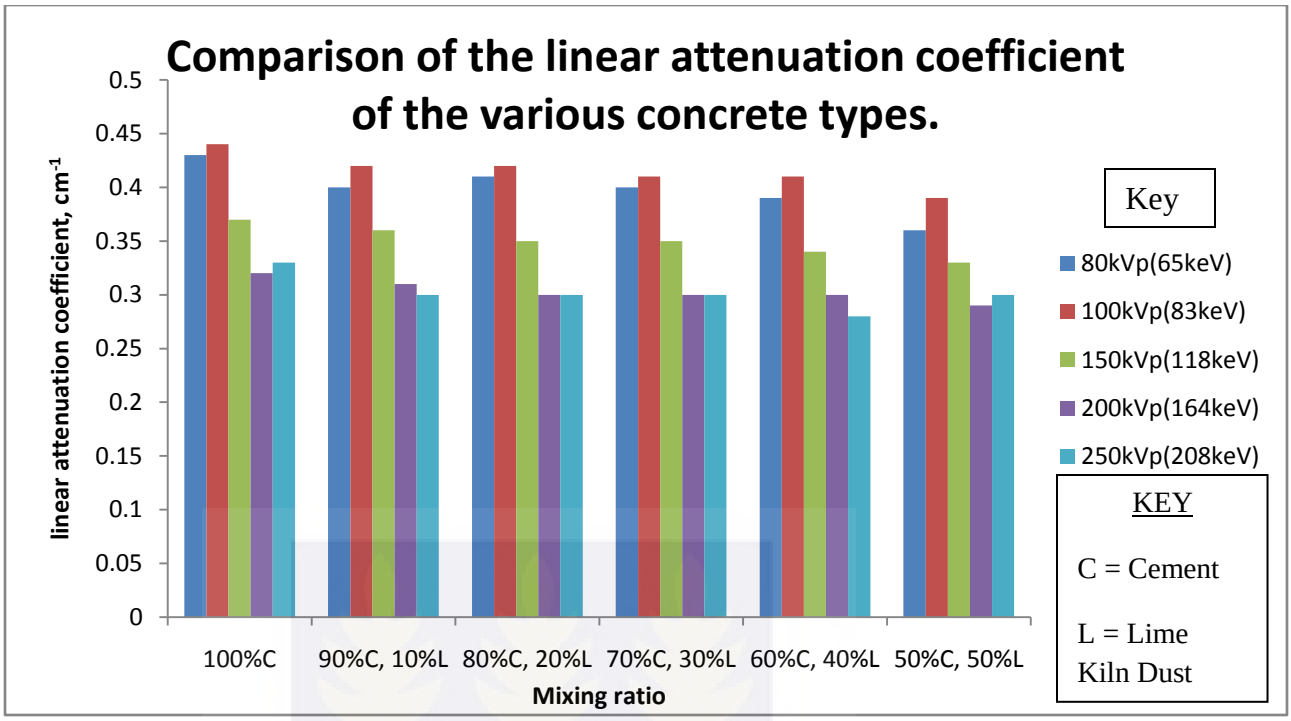

Figure 4.12: A plot of the various linear attenuation coefficients against the different mixing ratios for varying x-ray energies.

The linear attenuation coefficient, μ, is a constant that describes the unique properties of a material that attenuates a photon beam. It has units of cm^{-1}. Figures 4.6 – 4.11 show the attenuation curves of five (5) x-ray energies through the six (6) concrete types. For each concrete type, there is a plot of dose rate, which is the energy imparted in a medium, specifically concrete in this case, per unit mass per hour on the vertical axis and the concrete thickness on the horizontal axis.

For each x-ray energy through each concrete type, a line of best fit is plotted through the points and the equation of the line displayed. The equations for the respective attenuation curves are exponential functions which are in conformity with the theoretical equation

relating the initial incident radiation intensity to the final transmitted radiation intensity, absorber thickness and the linear attenuation coefficient given in equation (2.1).

Generally, as the concrete thicknesses of all the concrete types increase, the x-ray attenuation curves approach the axis of the thickness. Figure 4.12 summaries the various linear attenuation coefficients for the various mixing ratios corresponding to the x-ray energies.

Linear attenuation coefficient is derived from the x-ray's interaction with the material. The ability of concrete to attenuate x-ray intensity is assessed using its linear or mass attenuation coefficient. X-rays interact with concrete through two (2) main processes; Compton scattering and Photoelectric effect. The relative contributions of Compton scattering and photoelectric absorption are functions of the energy of the incident x-ray. In concrete, Compton scattering is the dominant process for x-ray energies in the range of 60 keV to 15 MeV, while photoelectric absorption dominates below 60KeV [75].

The amount of Compton scattering that occurs at a given x-ray energy is a function of the density of the sample been irradiated whilst the photoelectric absorption that occurs is primarily a function of the chemical composition of the sample and increases as the fourth power of the atomic number of the elements presents [75].

4.2.2 Mean Free Path (mfp)

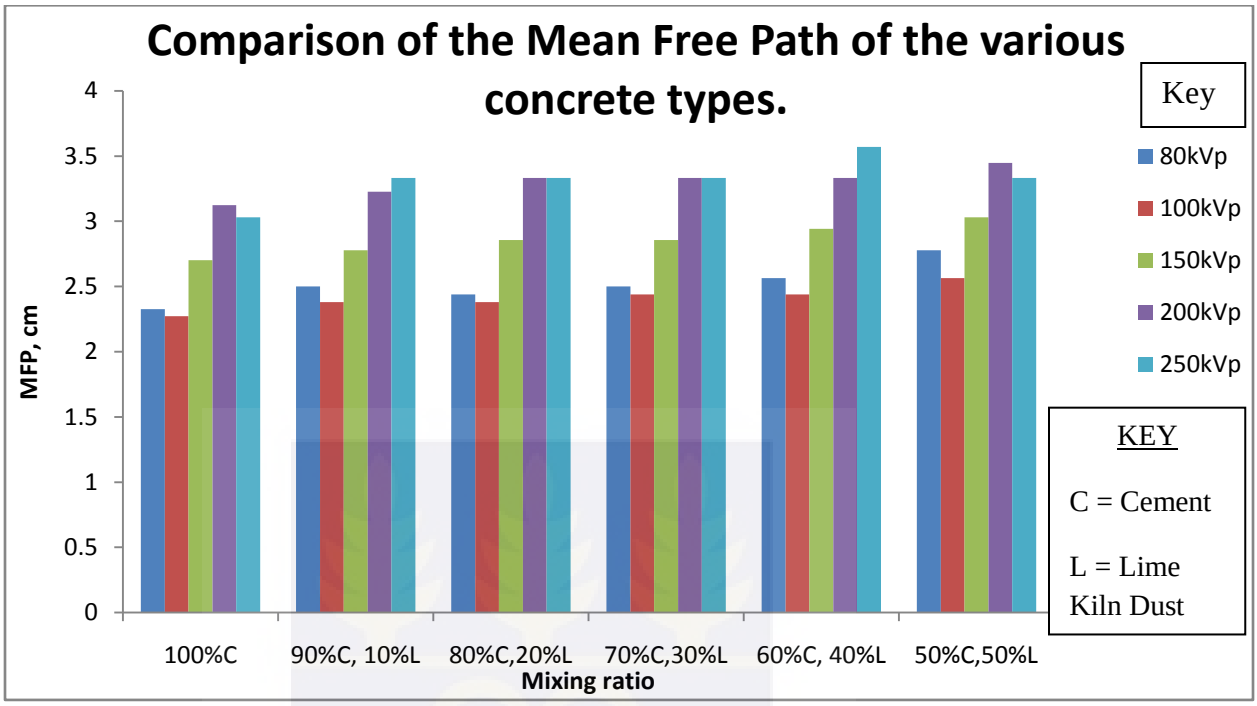

Figure 4.13: A plot of the mean free path against the different mixing ratios for varying x-ray energies.

Mean Free Path (mfp) is the average distance travelled by a photon between collisions. The collisions results in attenuation of the incident beam [4]. The more energetic the x-ray photons are and the denser the absorbing material, the more frequent the collisions become. As density increases, the molecules of the concrete become closer to each other. Therefore, the x-ray photons are more likely to run into the molecules of the concrete after travelling a short distance, so the mean free path decreases [76]. On the other hand, holding density of the concrete for each mixing ratio constant, the less energetic the x-ray photons produce a lower mfp value as compared to the mfp value for a higher energy for the same density of concrete. Energetic x-ray photons travel through the concrete

medium at a fast pace compared to less energetic photons, these results in less frequent collisions. Once the collisions are few, linear attenuation coefficient becomes low. This implies a long mfp, since an inverse relation exist between linear attenuation coefficient and mfp.

From figure 4.13, there is a general increase in the mfp as the density of the concrete reduces. The mfp for 100% concrete with a density of $(2.4557 \pm 0.0041e^{-3})$ gcm^{-3} is 2.3256 cm at 80 kVp whilst the mfp for 50% cement, 50% LKD concrete which has a density of $(2.3753 \pm 0.0221e^{-3})$ gcm^{-3} for the same energy is 2.7778 cm.

Table 4.6: Table of mean free path (cm) of the various concrete types with their respective density values quoted in gcm^{-3}

Peak Voltage (kVp)	100 % concrete (ρ =2.4557)	90 % C, 10% LKD (ρ =2.4622)	80% C, 20% LKD (ρ =2.4109)	70 % C, 30 % LKD (ρ =2.3743)	60 %C, 40% LKD (ρ =2.3773)	50 % C, 50% LKD (ρ =2.3753)
80	2.3256	2.5000	2.4390	2.5000	2.5641	2.7778
100	2.2727	2.3810	2.3810	2.4390	2.4390	2.5641
150	2.7027	2.778	2.8571	2.8571	2.9412	3.0303
200	3.1250	3.2258	3.3333	3.3333	3.3333	3.4482
250	3.0303	3.3333	3.3333	3.3333	3.5714	3.3333

Table 4.6 summarizes the mfp values for the various concrete types. Decrease in density results in an increase in the mfp value. For a concrete type with fixed density, lower energies of x-rays have a lower mfp value.

4.2.3 Mass attenuation coefficient, μ/ρ (cm^2g^{-1})

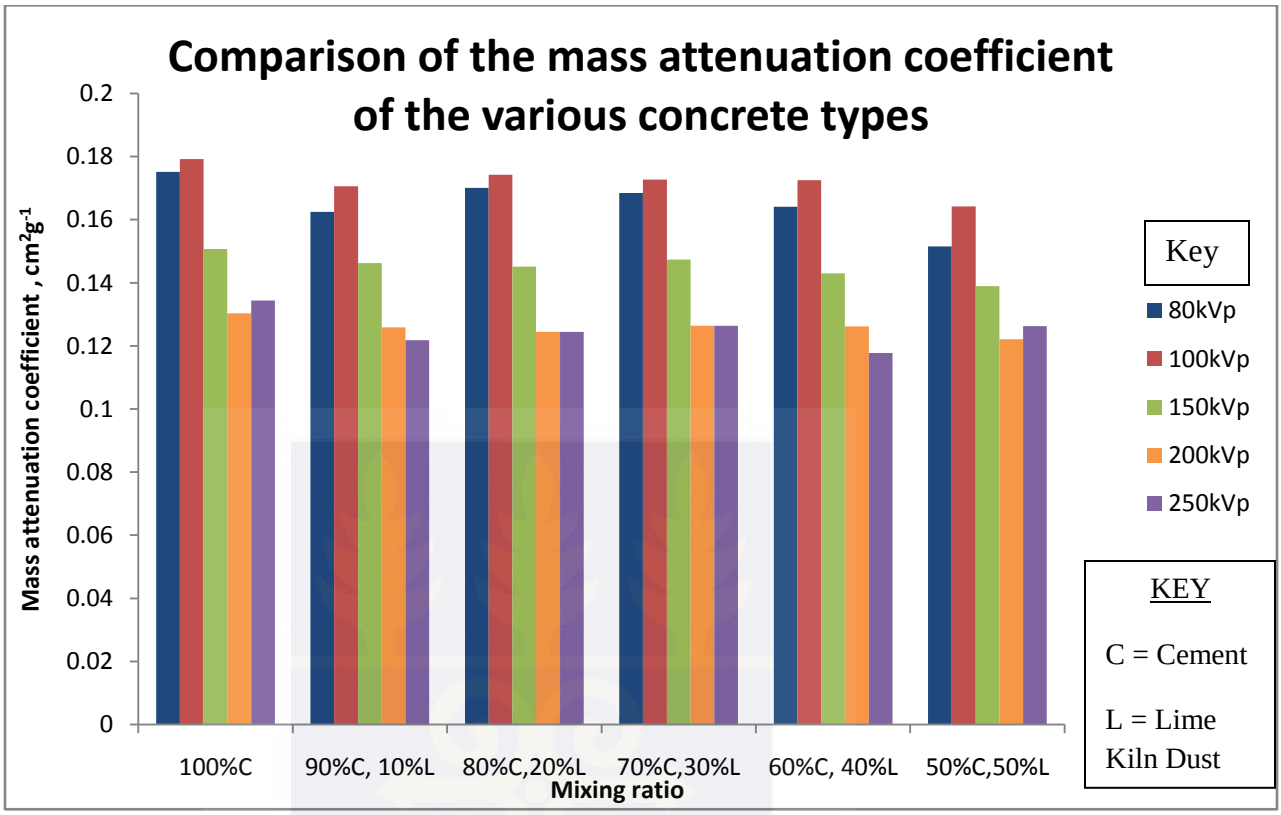

Figure 4.14: A plot of Mass attenuation coefficient against mixing ratio for all the x-ray energies.

Mass attenuation coefficient is one of the basic quantities used in calculations of the penetration and the energy deposition by photons (x-ray) in biological, shielding and other materials.

Linear attenuation coefficient reflects the removal of x-ray photons from a beam by interaction with electrons of the material probed, in this case concrete samples. The higher the electron density, the more interaction of x-ray photons with the sample material occurs. These interactions can be absorption of the photons (removal from the

beam) or scattering (change of direction with reduction in energy). It seems therefore appropriate to scale the linear attenuation coefficient with the sample density [77].

For a given thickness, probability of interaction is dependent on number of atoms per volume. Dependency can be overcome by normalizing linear attenuation coefficient for density of material.

The x-ray mass-attenuation coefficient of different concrete with varying composition of LKD was calculated at 5 different energies between 80 to 250 kVp. From the plot in figure 4.14, a general trend is observed. The observed trend is as energy increases for the respective mixing ratios, the value of the mass attenuation coefficient decreases.

Table 4.7: Table of mass attenuation coefficient (cm^2g^{-1}) of the various concrete types with their respective density values quoted in gcm^{-3}

Peak Voltage (kVp)	100 % concrete (ρ =2.4557)	90 % C, 10% LKD (ρ =2.4622)	80% C, 20% LKD (ρ =2.4109)	70 % C, 30 % LKD (ρ =2.3743)	60 % C, 40% LKD (ρ =2.3773)	50 % C, 50% LKD (ρ =2.3753)
80	0.1751	0.1624	0.1701	0.1685	0.1641	0.1516
100	0.1791	0.1706	0.1742	0.1723	0.1725	0.1642
150	0.1507	0.1462	0.1451	0.1474	0.1430	0.1389
200	0.1303	0.1259	0.1244	0.1264	0.1262	0.1221
250	0.1344	0.1218	0.1244	0.1264	0.1178	0.1263

Mass attenuation coefficient is highly dependent on the density of the attenuator (concrete) and the linear attenuation coefficient. Assuming the linear attenuation coefficient to be constant for the same energy, mass attenuation coefficient is highly dependent on the density of the concrete. A decrease in the density of the concrete and an increase in the linear attenuation coefficient, results in an increase in the mass attenuation coefficient for the same energy whilst a decrease in both density and linear attenuation coefficient results in a decrease in the mass attenuation coefficient.

From table 4.7, 100% concrete, ρ=2.4557 gcm^{-3}, has a mass attenuation coefficient of 0.1751 cm^2g^{-1} for 80 kVp and the mass attenuation coefficient for 50% cement, 50% LKD concrete, ρ=2.4557 gcm^{-3}, at the same energy is 0.1516 cm^2g^{-1}.

4.2.4 Half Value Layer, HVL

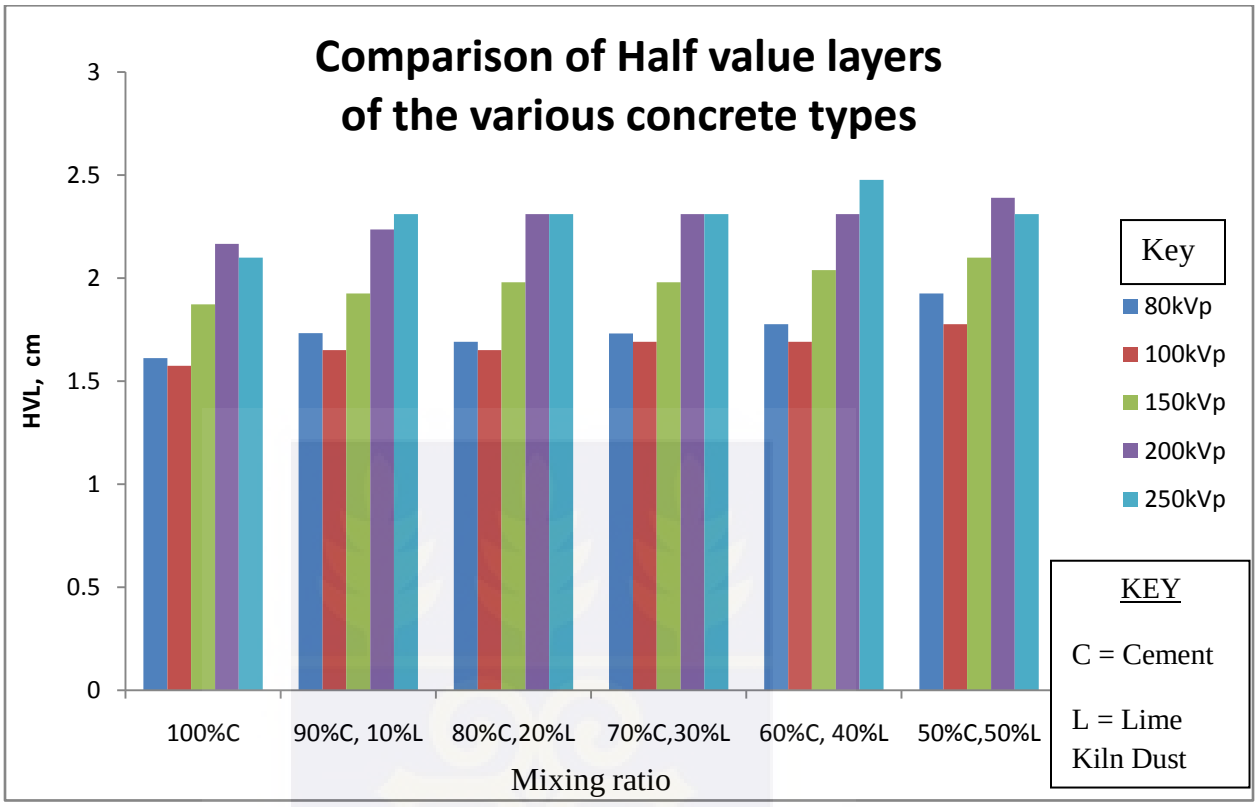

Figure 4.15: A plot of HVL against mixing ratio for all the x-ray energies.

The concept of half - value layer (HVL) is used to quantify the ability of an x - ray beam to penetrate the material being examined. The HVL of a material being traversed by an x - ray beam, is the thickness of absorbing material or filtration that must be placed in the beam to reduce the transmission of the beam by one half. HVL is dependent on the linear attenuation coefficient, μ as well as the density of the material.

From the plot in figure 4.15, there is a general increase in the HVL values as the energy increases for the different mixing ratios.

Table 4.8: Table of half value layer (cm) of the various concrete types, lead and ordinary concrete.

voltage (kVp)	Half-Value Layer, cm							
	A	B	C	D	E	F	G	H
80	-	-	1.6116	1.7325	1.6902	1.7325	1.7769	1.925
100	0.027	1.51	1.5750	1.6500	1.65	1.6902	1.6902	1.7769
150	0.03	2.232	1.8730	1.9250	1.98	1.98	2.0382	2.1
200	0.052	2.5	2.1656	2.2355	2.31	2.31	2.31	2.3897
250	0.088	2.8	2.100	2.3100	2.31	2.31	2.475	2.31

Where A is Lead with a density (ρ) of 11.35 gcm^{-3}, B is ordinary concrete with a density (ρ) of 2.3gcm^{-3}, C is 100% concrete (ρ = 2.4557 gcm^{-3}), D is 90% cement, 10% LKD concrete (ρ = 2.4622 gcm^{-3}) , E is 80% cement, 20% LKD concrete (ρ = 2.4109 gcm^{-3}), F is 70% cement, 30% LKD concrete (ρ = 2.3743 gcm^{-3}), G is 60% cement, 40% LKD concrete (ρ = 2.3773 gcm^{-3}) and H is 50% cement, 50% LKD concrete (ρ = 2.3753gcm^{-3}).

From table 4.8, Lead which has the highest density (11.35 gcm^{-3}) has an HVL value of 0.088 cm at 250 kVp. Ordinary concrete, (ρ = 2.3gcm^{-3}) has an HVL of 2.8 cm at the same kVp. HVL is dependent on both the density of the material as well as the linear attenuation coefficient. This statement is validated in the fact that even though 90% cement, 10% LKD which has a slightly higher density than 100% concrete and the rest of the mixing ratios, the HVL values for 100% concrete is appreciable than that of 90%

cement, 10% LKD. This is due to the linear attenuation coefficient value which is due to the interaction of the x-ray photons with the concrete.

4.2.5 Tenth Value Layer, TVL

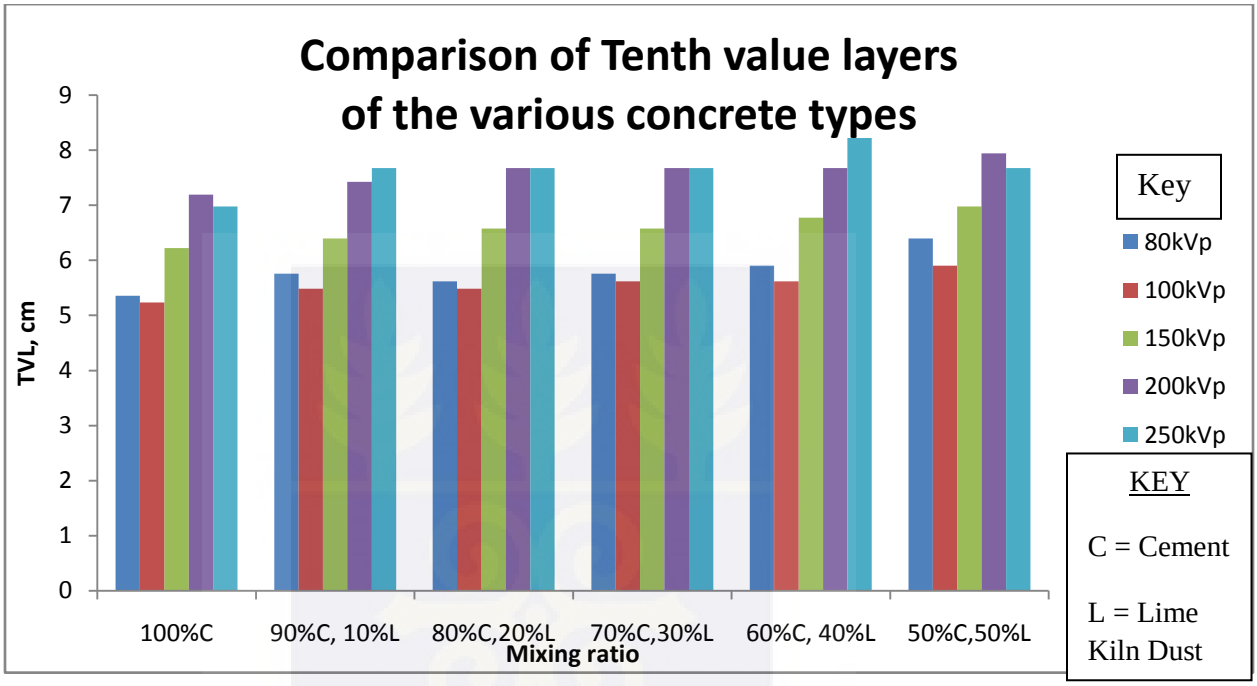

Figure 4.16: A plot of TVL against mixing ratio for all the x-ray energies.

Tenth value layer (TVL) is the shield thickness needed to reduce the intensity of the incident x-ray to 1/10th. The TVL is used in radiation protection to determine the number of thicknesses required for shielding. From the plot in figure 4.16, there is a general trend where an increase in energy and a decrease in density results in higher TVL values. 80 kVp is seen to have a higher TVL for all the concrete types than 100 kVp. This is as a result of the interaction of x-ray photons with the concrete which greatly influences the linear attenuation coefficient.

Table 4.9: Table of tenth value layer (cm) of the various concrete types.

voltage (kVp)	Tenth Value layer, cm					
	A	B	C	D	E	F
80	5.3549	5.7565	5.6161	5.7565	5.9041	6.3961
100	5.2332	5.4824	5.4824	5.6161	5.6161	5.9041
150	6.2232	6.3961	6.5789	6.5789	6.7724	6.9776
200	7.1956	7.4277	7.6753	7.67533	7.6753	7.9400
250	6.9776	7.6753	7.6753	7.6753	8.2236	7.6753

Where A is 100% concrete ($\rho = 2.4557 gcm^{-3}$), B is 90% cement, 10% LKD concrete ($\rho = 2.4622 gcm^{-3}$) , C is 80% cement, 20% LKD concrete ($\rho = 2.4109\ gcm^{-3}$), D is 70% cement, 30% LKD concrete ($\rho = 2.3743 gcm^{-3}$), E is 60% cement, 40% LKD concrete ($\rho = 2.3773 gcm^{-3}$) and F is 50% cement, 50% LKD concrete ($\rho = 2.3753 gcm^{-3}$).

Just like HVL, TVL is also dependent on density and linear attenuation coefficient.

Table 4.9 summarizes the TVL values for the various concrete types. The TVL values increase as the energy increases for a particular concrete type with a fixed density. 90% cement, 10% LKD concrete has a TVL value of 5.7565 cm for 80 kVp and 7.6753 for 250 kVp. Decreasing density increases the TVL for a fixed kVp. 80% cement, 20% LKD concrete ($\rho = 2.4109\ gcm^{-3}$) has a TVL of 7.6753 cm for 200 kVp whilst 50% cement, 50% LKD concrete ($\rho = 2.3753 gcm^{-3}$) produces a TVL of 7.9400 for the same 200 kVp.

This validates the statement that TVL and HVL are dependent on both density and linear attenuation coefficient.

The results and discussions have characterized the various concrete types investigated in this study and have given enough information based on which a valid decision of choice of concrete types can be made with respect to structural and shielding of x-rays.

CHAPTER FIVE

CONCLUSIONS AND RECOMMENDATIONS

Although there are many forms and types of radiation which may be injurious to health, the primary ones of concern are gamma rays, x-rays, and neutron particles. It is widely accepted that if adequate shielding is provided for these forms of radiations, the effects from the others can be considered negligible. This protection can be accomplished by barrier shielding with a material that will induce sufficient attenuation of the radiation intensity caused by a particular installation to a tolerable level.

As the final chapter of this thesis, the major outcomes are highlighted and summarized. Based on the outcomes, recommendations are accordingly made.

5.1 Conclusions

The main objective of this research work was to investigate the best composition mix of lime kiln dust (LKD), a by-product from the production of quicklime and hydrated lime by Carmeuse Lime Product Limited, Takoradi, as a component of concrete to determine its suitability and effectiveness for x-ray housing and shielding.

Specifically, the following enquiries needed to be made

- What are the major engineering (mechanical) properties the concrete produced by the addition of the varying percentages of LKD ranging from 10% to 50% of the cement constituent possess ?
- How well are they able to shield the x-rays in the selected energy range?

The above research questions have been well answered in this research work and the following conclusions have been arrived at.

1. The weight of the investigated concrete samples range from (8.288 ± 0.014) kg for 100% concrete to (8.016 ± 0.0746) kg for 50% cement, 50% LKD concrete.
2. The densities of the concrete samples range from (2.4557 ± 0.0041E-3) gcm^{-3} for 100% concrete to (2.3753 ± 0.0221E-3) $gcm^{-3}$for 50% cement, 50% LKD concrete. The average density for all the concrete types is (2.4093 ± 0.4089E-3) gcm^{-3}. The densities generally decrease as the LKD content is increased. 90% cement, 10%LKD concrete has a slightly higher density of 0.43% more than 100% concrete. The densities of 100% concrete, 90% cement, 10% LKD concrete and 80% cement, 20% LKD concrete are outside the range quoted in literature whilst the rest of the samples fall within range.

   This study also shows that even though slight addition of 10% LKD increases the weight and density of the concrete compared to regular concretes, further increases in the LKD content decreases the weights and densities.
3. The mechanical properties (compressive strength, flexural tensile strength and modulus of elasticity) generally decrease as the LKD content in the mix is increased.
4. All the graphs for the engineering properties followed a general trend. This was because
   i) Measured mass was used to calculate the density
   ii) Experimented compressive strength value was used to calculate other parameters

This is not surprising because each of them had inputs that followed the same trend. If each of the tests had been done experimentally, then maybe, some slight variations would have been noticed. The figures generally fall approximately within the accepted range.

5. The linear attenuation coefficient which describes the fraction of a beam of x-rays that are absorbed and/or scattered per unit thickness of an absorber is strongly linked to the density, elemental composition of the absorber and the energy of the incident x-ray photon. This value basically accounts for the number of atoms in a cubic centimeter (cm^3) volume of material and the probability of the x-ray photon been scattered and /or absorbed. Generally, attenuation coefficient of the concrete decreases with increasing energy as LKD content in concrete is increased.
6. 100% concrete with a density of (2.4557 ± 0.0041E-3) gcm^{-3} generally had the highest linear attenuation coefficient for x-ray energies studied ranging from 0.43 cm^{-1} to 0.33 cm^{-1} for the least energy 80kVp (65keV) to 250kVp (208keV).
7. Even though 90% cement, 10% LKD has a slightly higher weight and density than 100% concrete, the linear attenuation coefficient values of 100% concrete are better than 90% cement, 10% LKD concrete. This shows that, linear attenuation coefficient is not only dependent on the density of the absorber and the energy of the incident x-ray photon; it is also dependent on the elemental composition of the attenuator.
8. In conformity to theories, linear attenuation coefficient is inversely related to HVL, TVL and mfp. A higher linear attenuation coefficient ensures a smaller

shield thickness requirement to reduce the energy of the incident x-ray photon by half, one-tenth and a shorter travelling distance for the x-ray photons.

9. Mass attenuation coefficient, μ/ρ, is strongly inversely related to the density of the attenuator and directly proportional to the linear attenuation coefficient.

Based on all the foregoing, it is concluded that all the concrete samples can be used as x-ray shielding material. Based on all the results for attenuation and mechanical properties, it can be concluded that if attenuation is the sole consideration, then 100% concrete is the best because it requires less thickness. The other concrete types can also be used for shielding because the thickness requirements are less as compared to ordinary concrete. However, if extra strength is a desirable quality, then 100% concrete and 90% cement, 10% LKD concrete are preferable.

5.2 Recommendations

The following recommendations have been drawn based on the outcomes of the study.

- The investigated concrete types should be studied for their effectiveness for shielding other nuclear radiations such as gammas, betas and neutrons
- For x-ray facilities such as Hospitals and laboratories, LKD can be included in the cement mix used for plastering to form a multilayer which can aid in attenuation.

Finally, this research has been extremely successful as the results of the research have contributed to the knowledge database on concrete and admixtures as an x-ray shielding material.

REFERENCES

[1] Sprawls P, PhD, Radiation penetration, retrieved June 20, 2013 from the World Wide Web: http://www.sprawls.org/ppmi2/RADPEN/

[2] Attenuation, Wikipedia, retrieved June 20, 2013 from the World Wide Web: http://en.wikipedia.org/wiki/Attenuation

[3] Staff report of the federal radiation council (1960), Background material for the development of radiation protection standards.

[4] Martin E.J, Physics for radiation (2006): A handbook, Wiley-VCH Verlag GmbH & co. KGaA, Weinhiem. pp 367

[5] Shultis J.K, Faw E.R (2005), Radiation shielding technology, Review Article, Health Physics, Volume 88 Number 4.

[6] A guide to the use of lead for radiation shielding, Lead Industries Association Inc, New York.

[7] Radiation shielding, retrieved October 18, 2012 from the World Wide Web: http://encyclopedia2.thefreedictionary.com/Radiation+Shielding.

[8] Sprawls P, PhD, X-Ray Tube Heating and Cooling, retrieved November 20, 2012 from the World Wide Web: http://www.sprawls.org/ppmi2/XRAYHEAT/.

[9] Fan, W.C. (1996), Shielding considerations for satellite microelectronics, Nuclear Science, IEEE Transactions on Nuclear Science. (Volume:43 , Issue: 6).

[10] Ling C-T, Poon C-S, Lam W-S, Chan T-P, Fung K. K-L (2012), x-ray shielding properties of cement mortars prepared with different types of aggregates, Materials and structures.

[11] Walker R.L, Grotenhuis M (1961), A summary of shielding constants for concrete.

[12] X-rays, retrieved March 13, 2013 from the World Wide Web: http://www.teralab.co.uk/Experiments/X_Rays/X_Rays_Page1.htm.

[13] Engineering toolbox, concrete properties, retrieved January 24, 2013 from the World Wide Web: http://www.engineeringtoolbox.com/concrete-properties-d_1223.html.

[14] Adegoke J.A, Olowomofe O.G (2011), Dependence of attenuation of ionizing radiation on compression and geologic material (an application to x-ray shielding), Australian Journal of basic and allied Sciences, 5(10): 584 – 590.

[15] Mann W B, (1988), Radioactivity Measurements: Principles and Practices, England.

[16] Nathuram R, Photon attenuation characteristics of radiation shielding materials.

[17] National Council on Radiation Protection and Measurement (2005), Structural Shielding Design and Evaluation for Megavoltage X- and Gamma-Ray Radiotherapy Facilities, Vol. 151.

[18] Akkurt I, Basyigi C, Akkas A, Kılınçarsla S, Mavi B, Günoglu K (2012), Determination of Some Heavyweight Aggregate Half Value Layer Thickness Used for Radiation Shielding, Proceedings of the International Congress on Advances in Applied Physics and Materials Science, Antalya 2011, ACTA PHYSICA POLONICA A, Vol. 121, No. 1.

[19] Health physics society, what is radiation?, retrieved March 12, 2013 from the World Wide Web: http://hps.org/publicinformation/ate/faqs/whatisradiation.html.

[20] Olarinoye I.O (2011), Variation of effective atomic numbers of some thermo luminescence and phantom materials with photon energies, Research Journal of chemical sciences, Vol., 1(2).

[21] Materials used in radiation shielding, retrieved December 18, 2013 from the World Wide Web: http://www.thomasnet.com/articles/custom-manufacturing-fabricating/radiation-shielding-materials.

[22] Sprawls P, PhD, Interaction of Radiation with Matter, retrieved March 12, 2013 from the World Wide Web: http://www.sprawls.org/ppmi2/INTERACT/.

[23] Prasad Guru S, Parthasaradhi K, Bloomer W.D (1998), Effective atomic numbers for photo absorption in alloys in the energy region of absorption edges, Radiation Physics and Chemistry, Volume 53 Issue 5, Pages 449–453

[24] Hubbel, J.H (1977), Photon mass attenuation and mass energy absorption coefficient for H, C, N, O, Ar and seven mixtures from 0.1 keV to 20 MeV, Radiation Research, No 1, Vol 70, pp 58 – 81.

[25] Health physics society, Radiation Basics - Interaction Coefficients, retrieved December 18, 2013 from the World Wide Web: http://hps.org/publicinformation/ate/q1632.html.

[26] Half value layer, retrieved January 12, 2013 from the World Wide Web: http://www.ndt-ed.org/EducationResources/CommunityCollege/Radiography/Physics/HalfValueLayer.htm.

[27] Q.A. Collectible (2001), Sponsored by CRCPD's Committee on Quality Assurance in Diagnostic X-ray (H-7), Beam Quality: Total Filtration and Half-Value Layer.

[28] Sayala D, PhD, A report on the innovative Radiation shielding wall technologies for medical facilities.

[29] Lamarsh R.J, Baratta J. A (2001), Introduction to Nuclear Engineering 3 rd edition.

[30] IAEA (1973), Market survey for nuclear power in developing countries, General report, Vienna, IAEA.

[31] Stanford University (2010), Radiation Safety Manual, Environmental Health and Safety, Stanford University, Stanford California

[32] Siqi X (2008), A Novel Ultra-light Structure for Radiation Shielding, A thesis submitted to the Graduate Faculty of North Carolina State University in partial fulfillment of the requirements for the Degree of Master of Science Nuclear Engineering Raleigh, North Carolina.

[33] Lead, Wikipedia, retrieved November 27, 2013 from the World Wide Web http://en.wikipedia.org/wiki/Lead.

[34] Kakani S.L, Kakani A (2004), Material science, New age international (P) Limited Publishers, New Dehli.

[35] Brooklyn Public Library Files; 1999

[36] NCRP report No 34 (1970)

[37] Yusof Abdullah, Mohd R. Y, Azali M, Zaifol S, Abdullah N.E (2010), Cement – boron carbide concrete as radiation shielding material, Journal of Nuclear and related technologies, Vol. 7, No. 2.

[38] BS EN 197-1:2000, conformity evaluation, CEN TC 30

[39] Concrete mixing ratio, retrieved October 17, 2013 from the World Wide Web: http://www.renovationrobot.com.au/concrete/concretemixratio.html.

[40] Water – cement ratio, Wikipedia, retrieved October 17, 2012 from the World Wide Web: http//en.wikipedia.org/wiki/Water-cement_ratio

[41] Yüksel E, Berivan Y (2011), An investigation of x-ray and radio-isotope energy absorption of heavy weight concretes containing barite, Bull. Material Science, Vol. 34, No 1, pp 169 – 175.

[42] El-Sayed Abdo A, Kansouh W.A, Megahid R.M (2002), Investigation of radiation attenuation properties for Baryte Concrete, Journal of applied Physics 41, p 7512.

[43] Ogundare O.F, Ogundele S.A, Akerele O.O, Balogun F.A (2012), Low-energy broad-beam photon shielding data for constituents of concrete, Journal of applied clinical medical physics, Vol 13.

[44] Acevedo E.C., Serrato G.M (2010), Determining the Effects of Radiation on Aging Concrete Structures of Nuclear Reactors – 10243, WM2010 Conference, March 7-11,Phoenix.

[45] Gencel O (2012), Gamma and neutron shielding characteristics of concretes containing different colemanite proportions, Nuclear Science and Technology: 41-49 ISBN: 978-81-7895-546-9.

[46] Gencel O, Brostow W, Ozel C, Filiz M (2010), Concretes Containing Hematite for Use as Shielding Barriers, ISSN 1392–1320 materials science (MEDŽIAGOTYRA). Vol. 16, No. 3.

[47] Quapp J.W, Miller W.H, Taylor J, Hundley C, Leroy N (2000), DUCRETE: A Cost Effective Radiation Shielding Material, Paper Summary Submitted to Spectrum 2000, Sept 24-28, 2000, Chattanooga, TN

[48] Oates J.A.H (1998), Projet de. Lime and Limestone – Chemistry and Technology, Production and Uses. Wiley-VCH, ISBN 3-527-29527-5.

[49] High Calcium Hydrated Lime, retrieved September 4, 2012 from the World Wide Web: http://www.graymont.com/prod_high_calcium_hydrated.shtml.

[50] Zumdahl, Steven S. (2009). Chemical Principles 6th Ed. Houghton Mifflin Company. p. A21

[51] Halstead, P.E.; Moore, A.E. (1957). "The Thermal Dissociation of Calcium Hydroxide". Journal of the Chemical Society **769**: 3873.

[52] Calcium hydroxide, Wikipedia, retrieved June 25, 2012 from the World Wide Web: www.en.wikipedia.org/wiki/calcium_hydroxide.

[53] Material safety data sheet, Quicklime, According to directive 91/155/EEC modified by directive 2001/58/EC

[54] Calcination and production of quicklime, retrieved September 3, 2012 from the World Wide Web: http://gh.carmeusegroup.com/page.asp?id=60&langue=EN.

[55] Material Safety Data Sheet LIME KILN DUST

[56] Rich H.D, Hutchison R.K, neutralization, stabilization of combined refuse using lime kiln dust at high power mountain.

[57] Kucuk N, Cakir M, Isitman N.A (2012), mass attenuation coefficients, effective atomic numbers and effective electron densities for some polymers, Radiation Protection Dosimetry.

[58] Manohara S.R, Hanagodimath S.M, Thind K.S, Gerward L (2008), On the effective atomic number and electron density: A comprehensive set of formulas for all types of materials and energies above 1 keV, Nuclear Instruments and Methods in Physics Research B.

[59] Prasad S. G., Parthasaradhi K., Bloomer W. D (1998) , Effective atomic numbers for photo absorption in alloys in the energy region of absorption edges. Radiat. Phys. Chem.

[60] Bielajew, A.F. (2001), Fundamentals of the Monte Carlo method for neutral and charged particle transport, The University of Michigan Press.

[61] Briesmeister, J.F. (2000), MCNP-A general Monte Carlo N-particle transport code, Version 4C. Technical Report No.LA-13709-M, Los Alamos National Laboratory, New Mexico.

[62] O'Neill A.C (2006), Computer Simulations of Radiation Shielding Materials for Use in the Space Radiation Environment, A thesis submitted in partial fulfillment of the requirement for the degree of Bachelor of Science in Physics from the College of William and Mary in Virginia, Williamsburg, Virginia.

[63] Concrete technology in brief, retrieved January 28, 2013 from the World Wide Web: http://gdadhikari.com.np/?q=node/15.

[64] Nasvik J (2005), What Causes Efflorescence and How do You Remove it?, Concrete Construction.

[65] What is Efflorescence, retrieved January 28, 2013 from the World Wide Web: http://buellinspections.com/the-essence-of-efflorescence assessed on 28-01-2013.

[66] Compressive strength, Wikipedia, retrieved February 15, 2013 from the World Wide Web: http://en.wikipedia.org/wiki/Compressive_strength.

[67] Concrete in practice, what, why & how? NRMCA series, CIP 35- Testing compressive strength of concrete

[68] Prof. Nemati M. K, summary lecture on concrete: structure and properties, CM 510 – advanced construction methods and techniques, Department of construction management, University of Washington

[69] Safety Reports Series No. 47 (2006), Radiation protection in the design of radiotherapy facilities, IAEA, Vienna.

[70] Flexural strength, retrieved February 18, 2013 from the World Wide Web: (http://www.answers.com/topic/flexural-strength#ixzz2F6LQ0rNj.

[71] Concrete in practice, what, why & how? NRMCA series, CIP 16- Flexural strength concrete

[72] Singh Z. A, Ibrahim A, Tahir P (2010), Drying shrinkage characteristics of concrete reinforced with oil palm trunk fiber, International Journal of Engineering Science and Technology, Vol. 2(5), 1441 – 1450.

[73] Civil engineering portal, retrieved February 25, 2013 from the World Wide Web: http://www.engineeringcivil.com/modulus-of-elasticity-of-concrete.html.

[74] Cobb F (2009), Structural Engineer's Pocket Book, 2nd Edition. CRC press, Boca Raton London, New York, Washington D C.

[75] Malhotra V.M, Carino N.J, Handbook on non-destructive testing of concrete, 2nd edition, CRC press, Boca Raton London, New York, Washington D C.

[76] Mean Free Path, UCDAVIS CHEMWIKI, retrieved May 15, 2013 from the World Wide Web:http://chemwiki.ucdavis.edu/Physical_Chemistry/Kinetics/Rate_Laws/Gas_Phase_Kinetics/Mean_Free_Path.

[77] Schram R.P.C (2001), X-ray attenuation Application of X-ray imaging for density analysis, Petten.

APPENDICES

Appendix A1: Data sheet for mechanical properties

Concrete type	Average Mass (kg)	Density (g/cm^3)	Compressive Strength (MPa)	Flexural Tensile Strength (MPa)	Modulus Of Elasticity (MPa)
100% C	8.288	2.4557	27.3575	3.6613	24583.0668
90%C, 10%L	8.31	2.4622	23.6598	3.405	22861.43
80%C, 20%L	8.1367	2.4109	16.8082	2.8698	19268.9683
70%C, 30%L	8.0133	2.3743	7.8903	1.9663	13202.1486
60%C, 40%L	8.0233	2.3773	8.0425	1.9852	13328.87
50%C, 50%L	8.0167	2.3753	5.3889	1.625	10910.5821

Appendix A2: Shielding parameters for 100% concrete

	Thickness			
	A(mm)	B(mm)	C(mm)	D(mm)
	14.01	14.01	32.02	55.01
	15.01	15.01	33.01	54.01
	15.01	14.01	33.01	55.01
	14.03	15.01	32.01	54.01
	14.01	12.01	32.01	53.02
	16.04	18.01	33.01	55.02
	17.01	16.01	33.01	54.01
	12.02	13.03	32.01	54.01
AVERAGE	14.6425	14.6375	32.51125	54.2625
STD DEV	1.50622281	1.8443098	0.5331962	0.7061111
AVERAGE(cm)	1.46425	1.46375	3.251152	5.42625
STD DEV(cm)	0.1506	0.1844	0.0533	0.0706

thickness	80kVp	100kVp	150kVp	200kVp	250kVp
0	31.019866	30.173137	230.86648	70.07987	85.31316
1.46425	14.579866	20.153137	132.46648	45.1332	56.76649
2.928	14.246533	10.413137	79.346483	28.0132	38.13316
3.251152	12.946533	9.2298033	72.886483	24.12654	33.80649
4.715402	5.347866	4.65447	41.906483	16.10654	19.13982
5.42625	3.207866	2.9891367	29.499817	12.36654	14.19982
6.8905	1.3831993	1.54847	18.25315	7.648537	9.141822

100% concrete

kVp	μ	HVL	TVL	μ/ρ	mfp
80	0.43	1.6116279	5.3548837	0.1751028	2.325581
100	0.44	1.575	5.2331818	0.179175	2.272727
150	0.37	1.872973	6.2232432	0.1506699	2.702703
200	0.32	2.165625	7.195625	0.1303091	3.125
250	0.33	2.1	6.9775758	0.1343812	3.030303

Appendix A3: Shielding parameters for 90% cement, 10% LKD concrete

	Thickness of concrete slabs			
	A(mm)	B(mm)	C(mm)	D(mm)
	15.01	14.01	35.02	51.01
	15.01	16.01	34.01	54.01
	15.01	15.01	36.01	55.01
	15.01	15.01	35.01	57.01
	14.02	16.01	35.01	56.01
	15.01	15.01	34.01	56.01
	14.01	13.01	37.01	53.01
	15.01	15.01	36.01	52.01
AVERAGE	14.76125	14.885	35.26125	54.26
STD DEV	0.4606033	0.9910312	1.0347593	2.12132034
AVE.(cm)	1.476125	1.4885	3.526125	5.426
STD DEV(cm)	0.0461	0.0991	0.1035	0.2121

Thickness	80kVp	100kVp	150kVp	200kVp	250kVp
0	30.993027	30.419818	235.933212	70.37319	83.31313
1.476125	13.08636	18.939818	156.666545	46.75319	58.19313
2.964625	15.799693	10.926485	82.2198787	31.71985	39.45313
3.526125	10.613027	7.843818	70.413212	21.84652	32.38646
5.00225	4.15836	4.0544847	40.1398787	15.11319	17.26646
5.426	3.7696933	3.1311513	33.5198787	12.94652	16.01313
6.902125	1.75636	1.7391513	20.4465453	8.223852	11.0798

90% cement, 10% LKD concrete

kVp	μ	HVL	TVL	μ/ρ	mfp
80	0.4	1.7325	5.7565	0.16245634	2.5
100	0.42	1.65	5.482381	0.17057916	2.380952
150	0.36	1.925	6.3961111	0.14621071	2.777778
200	0.31	2.2354839	7.4277419	0.12590366	3.225806
250	0.3	2.31	7.6753333	0.12184225	3.333333

Appendix A4: Shielding parameters for 80% cement, 20% LKD concrete

	Thickness of concrete slabs			
	A(mm)	B(mm)	C(mm)	D(mm)
	18.01	17.01	35.01	56.06
	19.01	17.01	35.01	57.01
	19.01	17.01	34.02	57.01
	17.01	15.01	34.03	59.01
	18.01	16.01	32.05	58.01
	17.02	14.01	34.01	55.01
	19.01	16.01	35.01	55.01
	18.01	15.01	34.01	58.06
AVERAGE	18.13625	15.885	34.14375	56.8975
STD DEV	0.832602	1.125992	0.978263	1.459146
AVE.(cm)	1.813625	1.5885	3.414375	5.68975
STD DEV(cm)	0.0833	0.1126	0.0987	0.1459

Thickness	80kVp	100kVp	150kVp	200kVp	250kVp
0	32.09316	30.21322	234.0665	69.33317	82.90655
1.813625	12.71982	18.16656	123.6665	40.73317	51.02655
3.402125	12.19982	9.336557	70.21317	23.43317	33.13988
3.414375	11.41316	8.726557	68.29317	22.61317	31.65988
5.228	4.045156	4.017224	39.19983	14.28651	16.66655
5.68975	3.235823	2.777891	30.25983	12.03984	14.13322
7.503375	1.295156	1.376557	16.63317	6.759174	9.219884

80% cement, 20% LKD concrete

kVp	μ	HVL	TVL	μ/ρ	mfp
80	0.41	1.690244	5.616098	0.170061	2.439024
100	0.42	1.65	5.482381	0.174209	2.380952
150	0.35	1.98	6.578857	0.145174	2.857143
200	0.3	2.31	7.675333	0.124435	3.333333
250	0.3	2.31	7.675333	0.124435	3.333333

Appendix A5: Shielding parameters for 70% cement, 30% LKD concrete

	Thickness of concrete slabs			
	A(mm)	B(mm)	C(mm)	D(mm)
	14.01	18.01	36.01	57.01
	15.01	18.01	36.01	56.06
	15.01	18.01	36.03	56.01
	15.01	18.01	37.01	57.01
	14.01	17.01	37.01	57.01
	16.01	17.05	35.01	57.01
	14.01	17.01	34.01	57.01
	15.01	17.05	35.03	57.01
AVERAGE	14.76	17.52	35.765	56.76625
STD DEV	0.7071068	0.52405016	1.0337587	0.451535
AVE.(cm)	1.476	1.752	3.5765	5.676625
STD DEV(cm)	0.0707	0.0524	0.1034	0.0452

Thickness	80kVp	100kVp	150kVp	200kVp	250kVp
0	30.7264887	30.653227	244.7332	74.57985	88.29318
1.476	10.5464887	20.546561	153.1999	48.59319	61.65318
3.228	14.3864887	9.9232273	80.25985	29.99319	39.33318
3.5765	12.1531553	8.1312273	69.74652	23.28652	34.50652
5.0525	4.76315533	4.6912273	40.68652	16.07319	18.52652
5.676625	3.02915533	3.1645607	32.53985	12.80652	15.29985
7.152625	1.32515533	1.629894	21.06652	8.441853	10.85985

70% cement, 30% LKD concrete

kVp	μ	HVL	TVL	μ/ρ	mfp
80	0.4	1.7325	5.7565	0.168471	2.5
100	0.41	1.6902439	5.6160976	0.172682	2.439024
150	0.35	1.98	6.5788571	0.147412	2.857143
200	0.3	2.31	7.6753333	0.126353	3.333333
250	0.3	2.31	7.6753333	0.126353	3.333333

Appendix A6: Shielding parameters for 60% cement, 40% LKD concrete

	Thickness of concrete slabs			
	A(mm)	B(mm)	C(mm)	D(mm)
	15.01	16.01	34.01	57.01
	19.01	17.01	34.01	57.01
	16.01	17.01	35.01	57.06
	16.01	15.01	35.01	58.01
	14.03	19.01	37.01	60.01
	16.01	14.01	37.01	57.01
	21.01	18.01	34.01	57.01
	17.01	18.01	34.01	58.01
AVERAGE	16.7625	16.76	35.01	57.64125
STD DEV	2.248503	1.669046	1.309307	1.056591
AVE.(cm)	1.67625	1.676	3.501	5.764125
STD DEV(cm)	0.2249	0.1669	0.1309	0.1057

Thickness	80kVp	100kVp	150kVp	200kVp	250kVp
0	33.81326	32.80658	249.9999	75.85319	91.69986
1.67625	14.13326	20.20658	147.9999	51.49986	61.50652
3.35225	14.82659	10.81991	87.9999	30.13986	40.45986
3.501	12.37993	9.340577	81.6999	28.50652	37.55986
5.17725	3.993925	4.20191	45.7999	15.93319	18.76652
5.764125	4.518592	3.766577	34.1999	14.57319	17.71986
7.440375	1.607259	1.514577	19.6999	8.421857	12.61319

60% cement, 40% LKD concrete

kVp	μ	HVL	TVL	μ/ρ	mfp
80	0.39	1.776923	5.904103	0.164052	2.564103
100	0.41	1.690244	5.616098	0.172465	2.439024
150	0.34	2.038235	6.772353	0.143019	2.941176
200	0.3	2.31	7.675333	0.126194	3.333333
250	0.28	2.475	8.223571	0.117781	3.571429

Appendix A7: Shielding parameters for 50% cement, 50% LKD concrete

	Thickness of concrete slabs			
	A(mm)	B(mm)	C(mm)	D(mm)
	16.01	15.01	34.01	53.01
	16.01	15.01	33.04	52.01
	16.01	15.01	33.01	51.04
	16.01	13.03	33.04	52.01
	16.01	15.01	33.06	52.06
	16.01	14.01	33.01	53.01
	16.01	16.01	33.01	51.04
	15.01	14.02	33.01	52.01
AVERAGE(mm)	15.885	14.63875	33.149	52.024
STD DEV(mm)	0.353553	0.9100932	0.3485	0.7448
AVE.(cm)	1.5885	1.463875	3.3149	5.2024
STD DEV(cm)	0.0353	0.091	0.0349	0.0745

	Thickness	80kVp	100kVp	150kVp	200kVp	250kVp
	0	33.546507	32.86	252.13	77.4998553	92.3999
	1.5885	16.373173	22.133	149	50.0998553	61.8999
	3.052375	17.49984	11.407	93.68	35.1998553	42.2999
	3.314875	14.226507	9.8205	86.78	28.0998553	37.7999
	4.903375	6.9345067	5.2312	47.773	17.9998553	20.2999
	5.202375	5.74184	4.7485	47.373	16.8998553	19.0999
	6.790875	2.3385067	2.3759	24.907	10.3998553	13.0999

50% cement, 50% LKD concrete

kVp	μ	HVL	TVL	μ/ρ	mfp
80	0.36	1.925	6.3961	0.1516	2.77778
100	0.39	1.7769231	5.9041	0.1642	2.5641
150	0.33	2.1	6.9776	0.1389	3.0303
200	0.29	2.3896552	7.94	0.1221	3.44828
250	0.3	2.31	7.6753	0.1263	3.33333